A Theoretical Investigation Into Dynamic Neurological Disorders Caused By Thalamocortical Dysrhythmia

T H E S I S

presented to the Faculty of Arts

of

the University of Zurich

for the degree of Doctor of Philosophy

by

Jörn Henning Proske

of Germany

Accepted in the spring semester 2009 on the recommendation
of Prof. Dr. Lutz Jäncke and Prof. Dr. Daniel Jeanmonod

2009

Acknowledgements

I am thankful to my supervisors, Daniel Jeanmonod, Paul Verschure, and Daniel Kiper, and Lutz Jäncke for support, encouragement, supervision and useful suggestions throughout this research work. I am also indebted to the previous work by Ulysses Bernardet who developed many of the software tools used in this work.

I would also like to offer my regards to all of those who supported me in any respect during the completion of the thesis.

Contents

List of Figures

List of Tables

Chapter 1

Introduction

The thalamus is the prime gateway of information from periphery to neocortex. Situated in a central position in the brain (see Figure 1.1) it not only receives and relays all visual, auditory, somatosensory, and gustatory information, but is also involved in the relay of motor signals from the central to the peripheral nervous system [69]. Within this framework it has been suggested that the thalamus serves both the transduction of peripheral sensory information to the cortex [103] as well as being involved in covert selective attention [85, 84].

Apart from this classical view of thalamic function it has become apparent that the thalamus is involved in the generation of brain rhythms [122, 126]. Both its physiology as well as its anatomical location predispose thalamic neurons to engage in rhythmic oscillations with cortical areas (discussed in detail in Chapter 2) [39]. Furthermore it has been observed that thalamic lesions lead to a desynchronization of rhythmic oscillations in the brain marked by a suppression of organized EEG activity [131, 79, 96].

Whereas the functional relevance of such oscillations remains unclear, there is strong correlative evidence that oscillations are an important determinant of different states of arousal. For example, slow oscillations tend to dominate in drowsy states and non-paradoxical sleep whereas high-frequency oscillations are associated with states of wakefulness and arousal [74, 126].

There is substantial evidence both in vivo and in vitro that the thalamus is involved in the generation of rhythmic oscillations both of high and low frequencies during both sleep and arousal and is thus an important element of the generation of functional brain states [55, 121, 12]. For example, the rhythms classically observed in the sleeping mammalian cortex can be prevented by isolating the cortical mantle from the thalamus [11, 14].

Figure 1.1: MRI cross-section of the brain with thalamus marked by arrow.

1.1 Thalamocortical dysrhythmia

An interesting strand of evidence for the importance of thalamocortical interaction in functional brain states comes from the study of neurological disease.

For many years now seemingly disparate neurological symptoms have been linked to changes in the profile of brain oscillations under the conceptual framework of thalamocortical dysrhythmia (TCD) [62, 63, 77, 65, 76]. The dysrhythmic brain exhibits both changes on a network level, expressed by increases in synchronous activity in the theta and beta/gamma frequency bands (see Figure 1.2) [89, 129, 109], as well as physiological changes at the single cell level [71, 65]. Thalamic neurons are endowed with a number of special biophys-

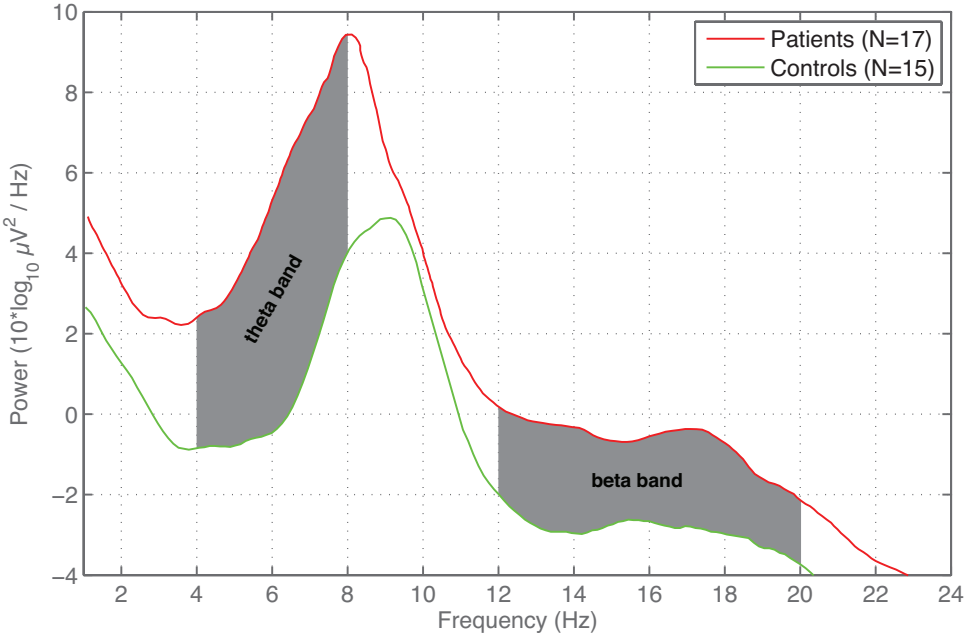

Figure 1.2: Comparison of EEG in TCD patients suffering from neurogenic pain and controls [111]. Synchrony is increased strongly in patients both in the theta and beta bands (shaded region).

ical properties that play an important role in the generation of brain rhythms [86, 121, 56]. At hyperpolarized levels of membrane potential these neurons switch from a tonic spiking regime to a burst spiking regime in which t-type calcium channels deinactivate and produce a large calcium spike upon release of hyperpolarization [75, 3, 31]. This calcium spike is then crowned by a series of sodium spikes occurring in quick succession. This behavior has been termed a calcium burst and has been shown to be a major component of the rhythms observed during non-paradoxical sleep and during states of drowsiness [126, 34]. Due to its relatively long refractory period and high synaptic efficacy bursts are ideally suited to recruit large ensembles of neurons in slow oscillations [33]. Lenz [71] and later Jeanmonod and colleagues [62] noticed a significant increase in the incidence of bursting thalamic neurons in patients suffering from chronic neuropathic pain.

The bulk of the bursting neurons Jeanmonod found were located in the posterior part of the central lateral thalamus - a region that is assumed to be involved in high-order multimodal processing [29]. The bursting thalamic neurons were

shown to be highly coherent in their activity to the observed changes in the EEG/MEG measures of patients suffering from a range of symptoms associated with TCD [112, 110, 109, 129].

While the process of bursting is completely physiological in the sleeping or drowsy brain [3, 122, 126], awake healthy states are characterized by a relatively small amount of bursting [74, 125, 120, 136]. The finding of a high incidence of bursting neurons in the thalamus of patients suffering from a wide range of neurological disorders lead subsequently to the hypothesis that these disorders are causally related to the appearance of bursts in awake brains [23, 100, 105, 90, 71, 62]. This notion was further corroborated by the finding that surgical lesions in the areas most affected by the bursting lead to beneficial effects in patients [71, 63, 50, 108].

Apart from the abnormal thalamic single cell recordings, there is converging evidence for secondary large-scale effects measured by EEG and MEG recordings in TCD patients [77, 76]. The power spectrum of oscillations compared between patients suffering from disorders associated with thalamocortical dysrhythmia and healthy age-matched controls differ significantly in both the theta band as well as the beta/gamma band (Figure 1.2). Detailed analysis of these differences revealed a high amount of coherence between the LFP recordings in the thalamus of patients and the theta changes in their EEG recordings[109, 129]. This lead to the hypothesis that thalamic bursts entrain cortical columns in low-frequency rhythms since thalamic bursting is known to occur at a frequency within the low-theta band [75].

In the light of this evidence a number of researchers suggested a chain of events connecting the physiological evidence with the observed symptoms under the term thalamocortical dysrhythmia (TCD) [63, 77]. It entails the following sequence of events: (1) A change of input to thalamic nuclei marked by either a lack of activation or overinhibition effectively hyperpolarizing thalamic neurons. This can be caused either internally by neurological disease or externally by insults to the peripheral nervous system. (2) Hyperpolarized thalamic neurons switch to burst mode that promotes the generation of low-frequency rhythmic oscillations in the functional thalamocortical module. (3) Lateral cortical disinhibition effects lead to cortical overactivation and the generation of positive symptoms [10].

The description of positive neurological symptoms as a consequence of unbalanced thalamocortical dynamics has gained much prominence in recent times [99]. It allows for an explanation for the success of functional neurosurgery in the treatment of seemingly disparate symptoms like Parkinson's tremor and neuropathic pain.

Recently, deep brain stimulation (DBS) of the subthalamic nucleus and the basal ganglia has yielded success in the treatment of a number of neurological symptoms [107, 135]. In DBS, a stimulation device is permanently implanted into the patients brain which is connected to a signal generator implanted in the patient's shoulder.

Ablative neurosurgical protocols in the treatment of thalamocortical dysrhythmia target the same system as DBS, albeit at a different level and following a somewhat different philosophy: one central mechanism can affect the subsystems of different modalities in the brain through the divergent thalamic efferent connections - producing unrelated symptoms characteristic of the affected domain. A permanent lesion in the thalamic areas producing the pathological rhythmicity readjusts the thalamocortical system towards a more physiological state and can relief the symptoms permanently [65]. In the face of the oftentimes extensive pharmaceutical history of patients this a very desirable outcome. Of course the irreversibility of the thalamic lesion compared to the DBS procedure requires a high amount of precision in pre-surgical planning and during the procedure.

Minimally invasive brain lesions by means of focused ultrasound (FUS) are now in the final stages of clinical testing. This new technique decreases the risks associated with invasive neurosurgery significantly. It is also possible to carry out online thermometry and to monitor every step of the lesioning process.

1.2 The connection of neuroscience and psychology

At the turn of the last century the study of the brain was segregated into anatomical, physiological and psychological sub-disciplines, each with its own methodologies and targets. In spite of significant advances in each of these areas there still remain gaps between these different levels of description that prevent a truly interdisciplinary approach to the big questions in neuroscience. Connecting the neuroscientific data of molecular, cellular, and systems processes in the brain to a behavioral level will be the challenge for the coming years.

Systems neuroscience is at the forefront of closing this gap and is directly connected to the microscopic molecular and cellular description levels. On the other hand, the study of small neuronal networks that has been conducted in systems neuroscience has also been hampered by the complexity it inherits from its underlying levels.

There are at present only two experimental methods that promise to shed

light on the void between the top-down and bottom-up approaches. Electrodynamic measures like electroencephalography (EEG) and magnetoencephalography (MEG) are well suited to look at correlations between large ensembles of neurons and allow the researcher to do so on a millisecond timescale. On the other hand, technological advances have enabled researchers to gain insight into hemodynamic measures like in functional magnetic-resonance imaging (fMRI). Here it is possible to gain a spatially more accurate insight at the cost of lower temporal accuracy. Whereas hemodynamic measures have much to tell about the underlying functional networks, electrodynamic measures allow for a description of how neurons interact dynamically in health and disease.

Connecting microscopic and behavioral descriptions of the brain is paramount especially in order to understand manifestations of neurological disease. As life-expectancy increases the WHO pinpoints neurological disorders as one of the greatest threats to public health in general [97].

Classically, the treatment of these disorders has been segregated into neurological and psychiatric disciplines. This is in direct correspondence to the dissociation of our current understanding of the brain mentioned above. A given symptomatology is either connected to our bottom-up or top-down understanding of brain function, ultimately neglecting any interaction between the two.

The interplay between physiology and psychology plays an important role especially in the domain of progressive neurodegenerative disease in which the affective dimension is a significant factor in the well-being of the patient [88]. Furthermore, many diseases considered essentially psychological have proved difficult to connect to a sound physiological footing. Examples are major depression, schizophrenia, obsessive-compulsive disorder, or addiction. In these disorders psychotherapy is an important part of the treatment plan but the accompanying pharmaceutical therapy is exclusively symptomatic.

The study of electrodynamic measures of the brain can allow researchers and doctors to use neural oscillations both as therapeutic as well as diagnostic tools in order to overcome the current physiological-psychological dissociation. Describing the disorders named above in terms of an underlying dysrhythmia can yield great power in unifying the psychological and physiological treatment domains and has proved to be successful in the face of failed conservative treatment. The consequences of reduced risks during surgery by means of the development of new non-invasive techniques such as FUS yields great promise for the future treatment of debilitating and oftentimes progressive neural disorders.

1.3 Outline

Functional neurosurgery as treatment for the dysrhythmic effects discussed above requires a basic understanding of the disease mechanisms that are to be controlled. So far, thalamocortical dysrhythmia has been described in terms of abstract models that are able to explain some of the features observed in TCD. These however do not have a numerical basis and are hence unable to produce testable predictions about the disease.

In this thesis I outline a computational model of thalamocortical dysrhythmia that extends the abstract model proposed by Jeanmonod and Llinas [63, 77].

In the following chapters I will address three important open questions in TCD theory:

In Chapter 3 I look at the generation of low-frequency rhythmicity in a single thalamocortical module. It is presently not clear which mechanisms translate hyperpolarization into rhythmic persistent bursting.

In Chapter 4 I demonstrate in a large-scale thalamic model consisting of different nuclei how the results from Chapter 3 hold up in the face of lateral interactions at the level of the thalamus. Furthermore, I provide an explanation for the importance of medial thalamic nuclei for the generation of physiological and pathological rhythms. The model also provides a number of important predictions regarding the efficacy of neurosurgical targets.

Lastly, in Chapter 5, I look at the generation of positive and negative symptoms in TCD. I show the numerical feasibility of unbalanced lateral cortical inhibition leading to over-activation surrounding TCD-affected areas (edge effect). I investigate what part of the parameter space is able to support such an activation pattern.

Chapter 2

The Thalamocortical System in Health and Disease

2.1 The anatomy of the thalamocortical system

The thalamus is a paired structure near the center of the brain (see Figure 1.1). It consists of 15-20 different nuclei, each with a distinct architecture and function. The nuclei of the thalamus can roughly be subdivided into three distinct groups. In the dorsal thalamus, there are the relay and associational nuclei as well as the nuclei of the intralaminar complex. The thalamic reticular nucleus is situated on the lateral side of each thalamic hemisphere [69].

Relay nuclei are more specifically innervated than the intralaminar and reticular nuclei [122]. They are often organized in a topographic fashion in correspondence with peripheral sources. Classic examples of relay nuclei are the lateral geniculate nucleus (LGN) in the visual domain, the medial geniculate nucleus (MGN) in the auditory domain, the ventral posterior complex (VPN) in the somatosensory domain, and the ventral anterior complex (VA) involved in motor control. Relay nuclei project to their specific sensory cortical areas and receive feedback from the same region they project to [113, 69].

In contrast, the intralaminar nuclei receive afferentation from a wide range of disparate sources [13]. Individual neurons tend to have large receptive fields and it is difficult to find correlates of specific functionality. These nuclei have hence been termed *non-specific* [114]. Classic examples of the intralaminar nuclei are the central lateral nucleus (CL) and the para-central nucleus (PC). Intralaminar nuclei project widely to different cortical areas [122, 46, 29]. The

same neurons tend to receive feedback from the areas they project to - therefore a certain specificity is preserved as in the relay nuclei [122].

The thalamic reticular nucleus is a sheet of cells situated around the dorsal thalamus. It is reciprocally connected with the underlying thalamic nuclei and consists exclusively of GABA-ergic neurons. In general, the reciprocal connections from the thalamic nuclei to the reticular nucleus and back tend to stay within domains with very little spread across the border of different thalamic regions [67]. That is, thalamic reticular neurons tend to project back to the same region they have been afferented from, within the thalamus [47, 67].

Thalamus and cortex form a tightly coupled system. All sensory, motor, and associational domains in the cortex are innervated by thalamic sources and reciprocally project back to the corresponding regions in the thalamus. Specific relay nuclei of the thalamus project to either layer IV or VI in the cortex [2]. These connections tend to be highly specific preserving the topography in sensory thalamic nuclei to the primary sensory cortices. In turn, neurons in layer VI project back to the thalamic nucleus afferenting to the same cortical microcolumn, thereby preserving a high amount of specificity in the reciprocal direction and closing a monosynaptic loop with the thalamus [51, 137]. This close coupling has lead to the proposition of so-called *thalamocortical columns* to be the basic functional building block of thalamocortical interaction, with closely circumscribed thalamic regions interacting with specific cortical columns [77, 69]. Both thalamocortical as well as corticothalamic fibers between the relay nuclei and cortex have axon collaterals to the reticular nucleus.

In contrast, the nuclei of the intralaminar complex project mainly to superficial cortical layers and these connections are not as specific as the connections from relay nuclei to the cortex mirroring the less specific innervation of thalamic intralaminar neurons [46, 29]. Also in contrast to the relay nuclei the corticothalamic fibers innervating the intralaminar complex do not collateralize to the reticular nucleus [114].

The architectural setup of thalamic neurons is depicted in a stylized fashion in Figure 2.1.

2.2 The physiology of the thalamocortical system

The thalamus albeit cell-physiologically more homogeneous than the cortex contains a number of different cell types, each endowed with different behaviors [68]. Most notable are the so-called thalamic relay neurons that receive affer-

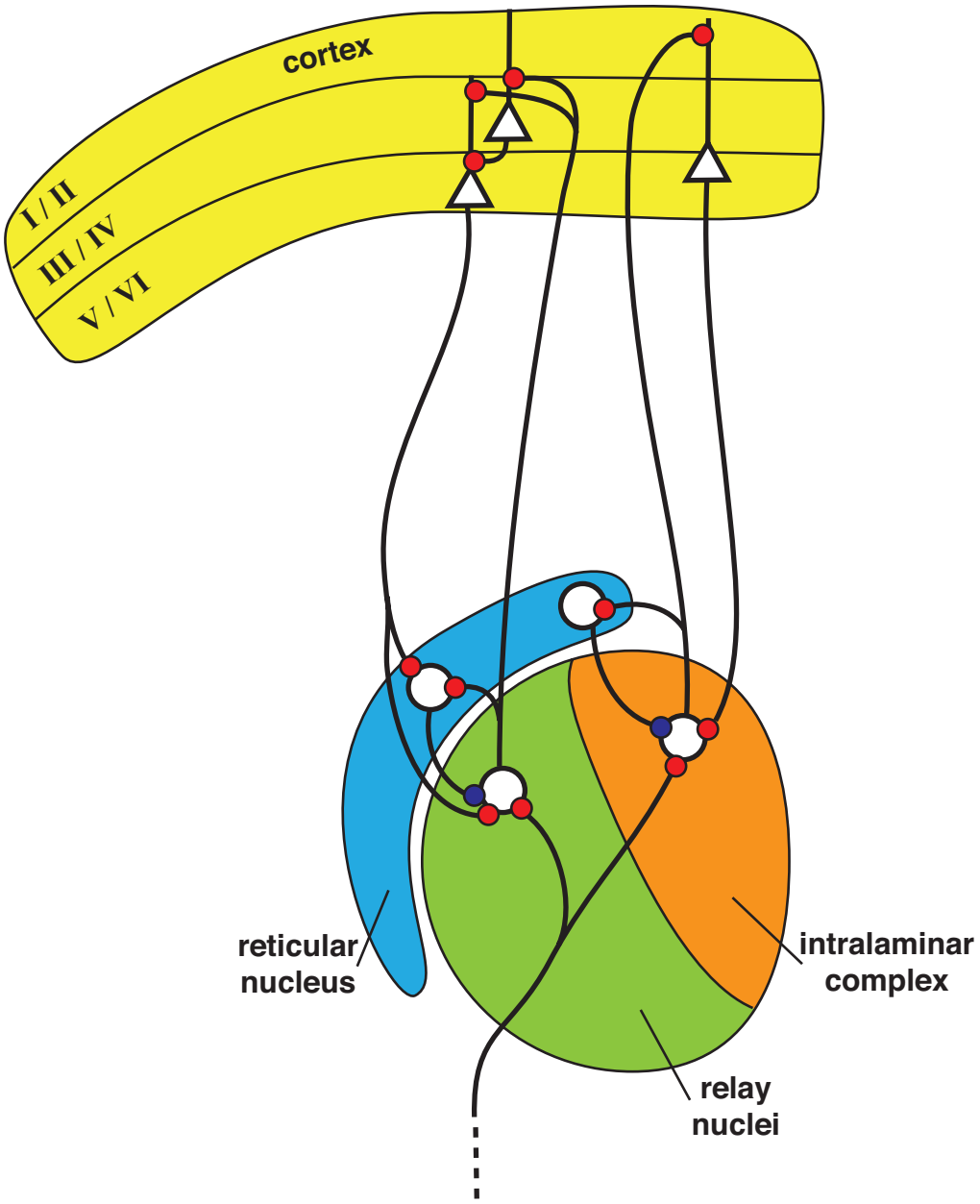

Figure 2.1: Stylized coronal view of a thalamocortical column, consisting of intralaminar nuclei (orange), relay nuclei (green), reticular nucleus (blue) and cortex (yellow). Synaptic connections between neurons (white) are marked with red circles for excitatory and blue for inhibitory connections.

ents from the periphery as well as the reticular nucleus and cortical layer VI [69]. These neurons fire in a tonic regime at relatively depolarized membrane potentials, i.e. their firing rate is proportional to the amount of depolarizing input they receive [75].

In contrast, at more hyperpolarized levels these neurons feature t-type calcium channels that obey a two-staged activation regime [75]. If the neuron is hyperpolarized beyond a certain level these channels deinactivate. This does not directly lead to a change in the neurons membrane potential. If the neurons get depolarized towards levels closer to the neuron's resting potential the channels activate and allow a massive influx of extracellular calcium. This leads to a strong depolarization of the neuron taking the neuron's membrane potential close to and above its firing threshold. Because of the temporal properties of the t-type channels this depolarization lasts longer than the depolarization carried by a conventional sodium spike [21, 22] and therefore allows the neuron to emit action potentials repeatedly with the after-hyperpolarization of the sodium spike being swallowed by the amplitude of the calcium depolarization [61].

This basic mechanism of dual firing regimes is also present in the neurons of the thalamic reticular nucleus [124]. Whereas some of the parameters differ, both thalamic relay and thalamic reticular neurons can fire tonically at depolarized levels of membrane potential and can emit calcium-mediated bursts if they become more hyperpolarized. The t-type calcium channels found in the reticular neurons tend to run on a slightly longer time scale than the channels in the thalamic relay neurons leading to overall longer bursts [57]. Whereas a typical burst in a thalamic relay neuron carries between 4 and 8 spikes this number is easily doubled by the neurons in the thalamic reticular nucleus. As will be seen below, these physiological properties of thalamic neurons are essential for the recruitment of large-scale persistent oscillations in the thalamocortical system.

2.3 The physiology of neural oscillations

Rhythmic fluctuations can be found in many systems in different disciplines on the macroscopic as well as the microscopic scale: finance, sociology, physics and biology. They serve as a control mechanism enabling stability in dynamical systems.

Neural systems are no exception. Since the first electrical recordings from the human scalp were published in the 1920s [9], the analysis of oscillatory patterns in the activity of the brain has been a successful research tool in the manifestation of electroencephalography (EEG), magnetoencephalography (MEG), as well as local field potentials (LFP) recorded invasively. Analysis of such

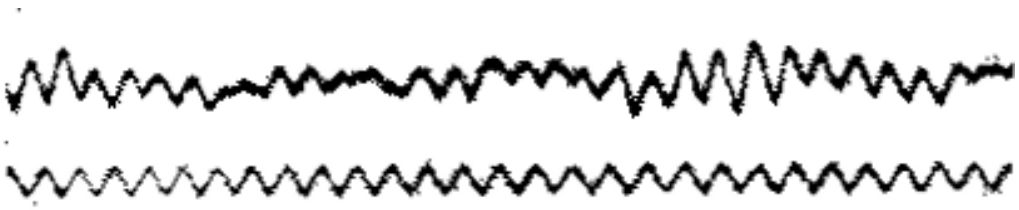

Figure 2.2: An early EEG recording obtained by Hans Berger [9]. The upper trace represents the recording of alpha activity and can be compared to the lower 10 Hz timing signal.

recordings has yielded a close correspondence between the frequency bands in which oscillations occur and general states of the brain, such as attention, sleep, epilepsy, coma, and anesthesia [6].

2.3.1 Synchrony

The potentials that can be measured on the scalp of subjects are based on the extracellular currents that compensate for the in and out-flux of ions through the membrane of individual neurons. These currents are extremely small and thus only show up when many neurons change their membrane potential in unison. An EEG wave is hence always an indication for synchronization between large numbers of neurons. This can occur as the result of external stimulation in the case of so-called evoked potentials [6]. Here the external stimulus is the synchronizing event that excites a large number of neurons and can then ripple through the system as a traveling wave.

However, there are also oscillations that are rhythmic and occur spontaneously, for example during slow-wave sleep [24, 26, 27, 126]. Here, there is no obvious synchronizing event indicating that these oscillations are based on intrinsic network interactions.

2.3.2 Functional relevance of different frequency bands

Rhythmic oscillations can occur at various frequencies, from the very slow delta (0-4Hz) to the very fast gamma bands (up to 100Hz) (see table 2.1). When analyzing power spectra from the human EEG it becomes apparent that generally an inverse relationship between the amplitude and the oscillation frequency (see Figure 2.3) holds. This indicates that for fast oscillations smaller groups of cells are recruited than for slow oscillations [17].

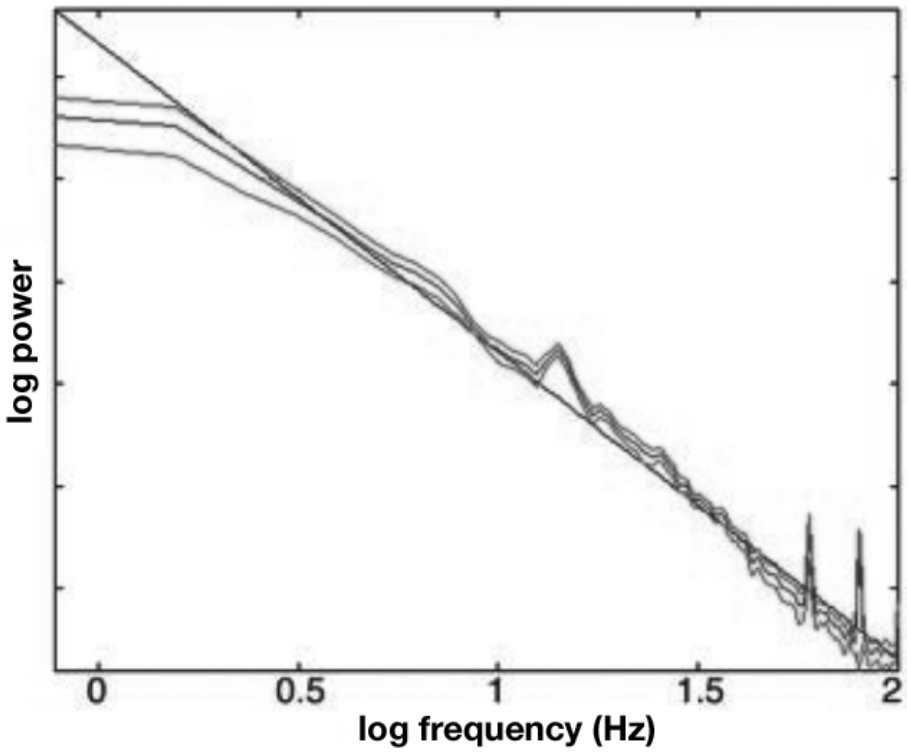

Figure 2.3: The powerspectrum of a subdural EEG recording from a sleeping human subject shows a linear decrease of log power with increasing log frequency. From [17].

The identification of functional correlates to certain oscillation frequencies has lead to the proposal of the delta, theta, alpha, beta, and gamma frequency bands. As more data has become available each of these bands has been further subdivided. It is important to realize that these bands are just labels used for the researcher's convenience:

Delta oscillations

The slow delta frequency-band is observed during slow-wave sleep but also during anesthesia and coma. It has been suggested that delta oscillations are produced by thalamocortical circuits. Blocking GABA receptors in the reticular nucleus of the thalamus leads to delta oscillations in in vitro preparations most likely due to an increase in reticular burst length followed by activation of

Name	Frequency (Hz)	Function
delta	0-4	especially prominent in slow-wave sleep and young infants
theta	4-8	prominent in young children, drowsiness
alpha	8-12	relaxation, eyes closed
beta	12-30	active concentration, alertness, motor function
gamma	30-100	cognitive function

Table 2.1: Frequency bands of neural rhythmic oscillations. Note, that there is no absolute agreement about the exact extend of each frequency band [9].

GABA-B receptors in the thalamic relay [80, 70].

Theta oscillations

In healthy subjects theta oscillations occur prominently in the limbic system, the entorhinal cortex and the hippocampus especially during arousal.

Alpha oscillations

Alpha activity is observed particularly over occipital areas in states of relaxation and when participants close their eyes. The alpha peak is the most prominent feature of the human EEG spectrum and accordingly was the first to be recognized by EEG pioneers [9].

High frequency oscillations

Beta and gamma oscillations are less obvious in EEG data. This is an indication that smaller groups of neurons are involved in the phase-locked oscillation. In general, high-frequency oscillations are considered to be more desynchronized but invasive recordings have revealed that on a local scale synchronization takes place and might be connected to cognitive function, especially focused attention [104] and performing complex motor tasks [92]. Futhermore, synchronous activity, especially high frequency bands, has been suggested to be responsible for cognitive binding [116, 41, 45], or might even be involved in forming population codes [138, 139, 130].

It is important to note that the EEG can show oscillations in many of these frequency bands at the same time. It is thus highly likely that interactions between different oscillatory sources can occur. Local oscillators might be coupled over long ranges and thus influence each other to produce phase-locked global oscillations. Also, it is likely that both sub-cellular as well as network mechanisms drive oscillations in the brain.

2.3.3 Generation of neural oscillations

Every oscillation is a result of delayed negative feedback [17]. These can be found on many different levels in the brain. On the smallest scale, voltage-gated ion channels can implement such a delayed feedback [53]. For example, during a spike, depolarizing sodium influx will be overcome by an outwards potassium current that re-hyperpolarizes the neuron. Under constant excitation this cycle will reoccur rhythmically. There are many examples of such channel-interactions on a single cell level [86, 75].

On a network level, the delayed negative feedback can be mediated by neurons interconnected with excitatory and inhibitory synaptic connections. In this case the oscillation is an emergent property of the network architecture [60, 132]. In local cortical networks there is a balance between these excitatory and inhibitory connections [140]. Activity of excitatory neurons will invariably excite inhibitory neurons that then mediate the delayed inhibition. The frequency of the oscillations thus depends both on the time-scale of excitation and inhibition as well as the delay between neurons.

In both cases, intrinsic and network oscillations, interactions can take place [118].

2.4 The thalamocortical system in TCD

2.4.1 Different manifestations of TCD

Symptoms caused by thalamocortical dysrhythmia can roughly be subdivided into positive and negative symptoms [10]. Negative symptoms arise out of the deafferentation or overinhibition of thalamocortical circuits that lead to an entrainment of thalamocortical modules into low-frequency theta rhythms. Positive symptoms are then an expression of the cortical excess activation caused by lateral disinhibition which has been called the edge effect [78, 77].

Neurogenic pain

Chronic neurogenic pain as caused by peripheral lesions to afferent nerve fibers or by lesions on the central pain pathways was the first disorder recognized to be implicated with thalamocortical dysrhythmia [71]. The deafferentation resulting from a peripheral insult subsequently leads to a lack of excitation in the thalamus leading to hyperpolarization of thalamic neurons. Pain is considered a positive symptom and hence requires the involvement of cortical interactions to generate overactivation in areas of the pain matrix.

Parkinson's Disease

Dopamine depletion in the basal ganglia leads to an overactivation of the globus pallidum internum (GPi) and hence a strong inhibitory input to ventral anterior and ventral lateral (VA/VL) thalamic areas. This can lead to a hyperpolarization of these nuclei. The connection between the occurrence of bursting neurons in the awake ventroanterior thalamus of patients suffering from tremor has been recognized for quite some time and the resulting oscillations have been implicated with the generation of tremor [20, 18, 19] outside a TCD context.

Tinnitus

Tinnitus has not received a lot of attention yet. Nevertheless, a number of interesting studies have been carried out concerned with tinnitus patients and their EEG compared to healthy controls. It is also possible to transiently relieve tinnitus by the presentation of a suitable auditory masking stimulus. This has been shown to concurrently normalize the patients EEG lending further support to the validity of the TCD concept [78].

Epilepsy

The symptoms described above are caused by peripheral changes to the input statistic to the thalamus. The epileptic TCD manifestation (similarly to central neurogenic pain) can be characterized caused by a top-down effect. Changes in the corticothalamic afferent input cause similar hyperpolarization in thalamic neurons. This can either be mediated by the direct corticothalamic connections or indirectly via corticoreticular connections that lead to strong inhibition in thalamic relays.

Neuropsychiatric disorders

Some disorders that have formerly been associated with the domain of psychiatry have also been shown to correlate with thalamocortical dysrhythmia, for example, major depression, obsessive-compulsive disorder (OCD), and schizophrenia. The underlying trigger in these manifestations of the disease are changes in the afferent input from limbic and paralimbic cortical areas to high-order multimodal thalamic nuclei.

2.4.2 The treatment protocols for TCD

The different manifestations of TCD can require different surgical targets:

CLT

In centrolateral thalamotomies, the central lateral nucleus of the thalamus is the target of choice against a wide range of dysrhythmic manifestations, most notably neurogenic pain, but also tinnitus, neuropsychiatric disorders and epilepsy [65]. In pain patients it achieves a 50-100% relief in 53% of the patients [63, 64].

PTT

Pallido-thalamic tractotomies target the fiber bundle connecting the globus pallidum to the thalamus. In Parkinson's Disease the inhibitory output nuclei of the basal ganglia are overactive and strongly inhibiti thalamic neurons of the VA/VL nuclei. During the PTT the connections from the basal ganglia to the thalamus are severed as completely as possible hence shutting off this overinhibition. Analysis of symptom relief in patients suffering from PD after surgery reveals a 65% improvement on the UPDRS scale. Furthermore, medication could be reduced by 52% overall, leading to termination of the pharmaceutical treatment in a third of the patients. [5, 82]

AMP

The anteromedial pallidotomy targets the pathway between the paralimbic internal pallidum and paralimbic parts of the thalamus and is indicated as an additional measure in the treatment of TCD-related neuropsychiatric disorders [65]. Surgical outcomes are more complex to evaluate in this domain, but case reports have shown promising results.

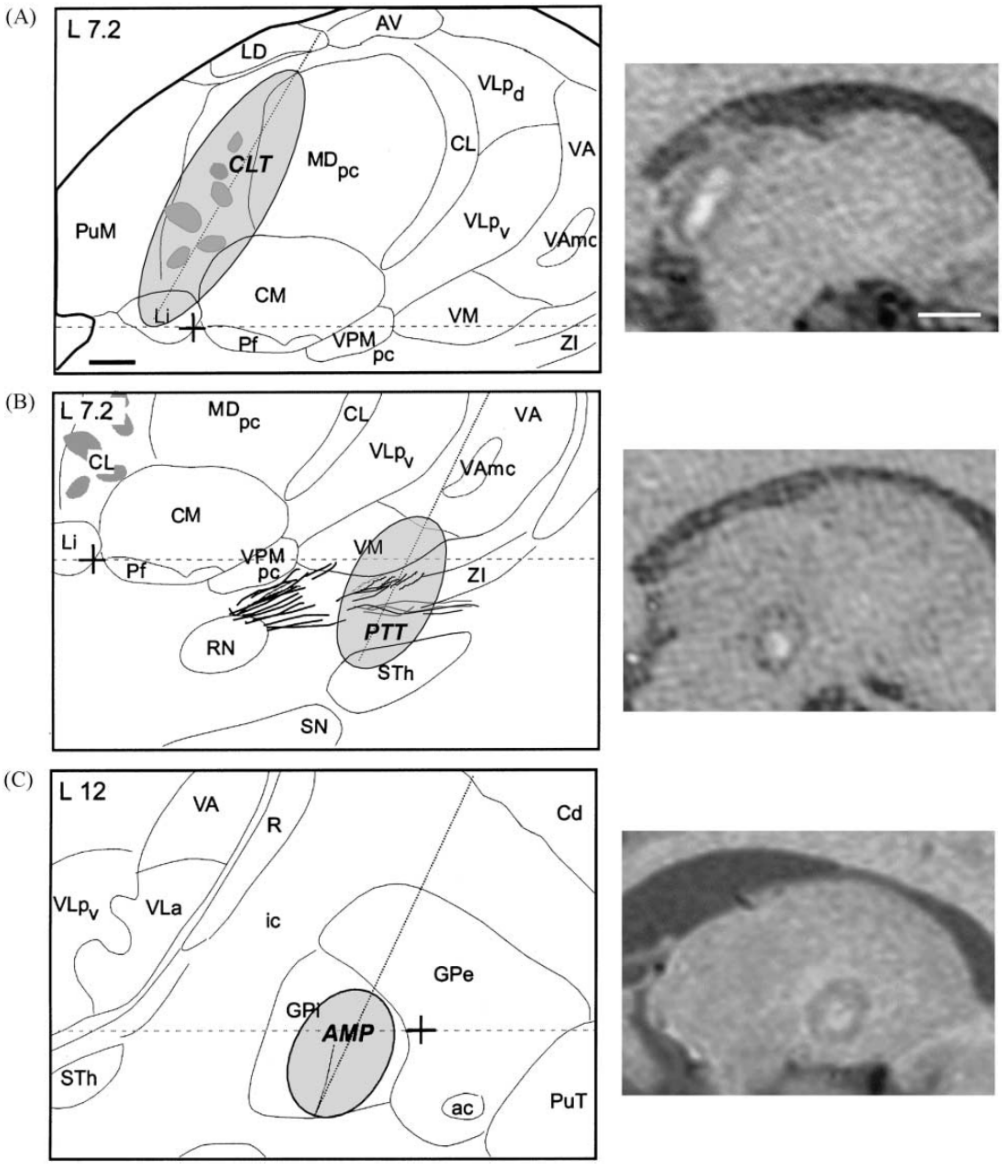

Figure 2.4: Atlas projections and post-op MR of CLT (a), PTT (b), and AMP (c). Cell clusters in CL are shown in dark gray. Scale bars (Atlas: 2mm, MR: 10mm). From [65]

Psychotherapy

There is converging evidence that emotional activity can lead to the production of low-frequency rhythmicity in humans [52, 81], much in the same way as in chronic pain and parkinson patients. This corroborates the notion that psychological and physiological processes are intertwined at the level of rhythmic oscillations in the brain.

It has been hypothesized that TCD can therefore be viewed as either a disorder caused by external factors or internal psychogenic factors that change the thalamic input [65].

Clinically, the need for a holistic treatment of patients with psychotherapeutical measures being applied alongside conventional pharmaceutical and surgical treatment has been emphasized [65]. Oftentimes the functional neurosurgery can only relief symptoms incompletely with symptomatic shifts from motor/somatosensory to emotional/psychological domains. There is hence the need to address both externally and internally-triggered TCD alike in order to achieve an optimal therapeutic effect.

2.4.3 Side effects of functional neurosurgery

The surgical procedures described above do not show significant long-term side effects [65]. This has been argued to be due to the fact that functions formerly carried out by the targeted areas have been plastically relocated by the brain over the course of the disease. There is an initial change in sleep patterns in patients after surgery which is completely reversed after a couple of weeks [106].

Chapter 3

Mechanisms of Persistent Low-frequency Bursting

3.1 Introduction

The thalamus and cortex form a tightly coupled dynamical system [119]. Under normal conditions this system tends to be in a stable state. In thalamocortical dysrhythmia changes in the activity of a small part of this system introduce an element of instability and make the system transition to a different state characterized by the genesis of positive symptoms such as chronic neuropathic pain, Parkinsonism, and tinnitus.

In this chapter I take a closer look at what factors are responsible for such a state transition. Furthermore, I investigate how different elements contribute to generate the physiological footprint apparent in patients.

3.1.1 The physiology of TCD

Certain physiological changes accompany the transition from the healthy to the dysrhythmic brain. First and foremost there is a strong tendency of thalamic neurons to emit bursts of action potentials [71, 63]. These bursts are generally implicated with states of sleep and drowsiness but are present in large numbers in the awake dysrhythmic brain. The discovery of these bursts in patients suffering from chronic pain was in fact imperative in the development of functional neurosurgical protocols for the treatment of pain and also the first piece of evidence for the existence of dysrhythmic syndromes in the brains of patients [62]. The existence of these bursts has been confirmed by extracellular recordings during functional neurosurgery for neurogenic pain as well as Parkinson's

disease, tinnitus, major depression, and epilepsy [65]. Sample traces of extracellular recordings from patients are shown in Figure 3.1.

LTS bursts

Llinas and Jahnsen were the first to investigate the mechanism of burst production in thalamic neurons [75]. They found that the sodium spikes that generated the high-frequency repeated action potentials in a thalamic burst were riding on a large-amplitude calcium depolarization mediated by t-type calcium channels. These channels underly a two-stage activation mechanism. They are deactivated at depolarized levels of membrane potential. This allows thalamic neurons to fire tonically in healthy, awake conditions. If a thalamic neuron gets hyperpolarized t-type calcium channels slowly start to deinactivate. A release from this hyperpolarization can then lead to the activation of the channels and hence to a massive influx of calcium that constitutes the wave observed in thalamic bursts. This release can happen passively at the offset of an inhibitory stimulus or in response to active depolarization by some sort of excitatory input.

The behavior of thalamic neurons can be understood in terms of three independent threshold levels in relation to the neurons' resting potential [117]. The lowest threshold is the calcium channel deinactivation threshold. The membrane potential needs to be below this threshold for the burst-producing calcium channels to start deinactivating.

At slightly higher levels of V_m lies the activation threshold that needs to be crossed to emit a burst. Note, that this only happens if enough calcium channels are deinactivated.

Yet higher lies the spiking threshold. The neuron's membrane potential needs to cross this threshold in order for action potentials to occur.

LTS bursts in TCD

The characteristic behavior described above has prompted researchers to derive the existence of abnormal membrane potential levels in the thalamus of patients suffering from thalamocortical dysrhythmia [63, 77]. Indeed, when looking at the symptoms associated with TCD it becomes apparent that all have in common a potential change in the input to the thalamus. Neurogenic pain is often caused by damage to the peripheral nervous system. Damaged nerves cannot carry excitatory input to the thalamus any more and hence it is feasible that thalamic neurons can become hyperpolarized enough under these conditions to warrant the deinactivation of t-type calcium channels.

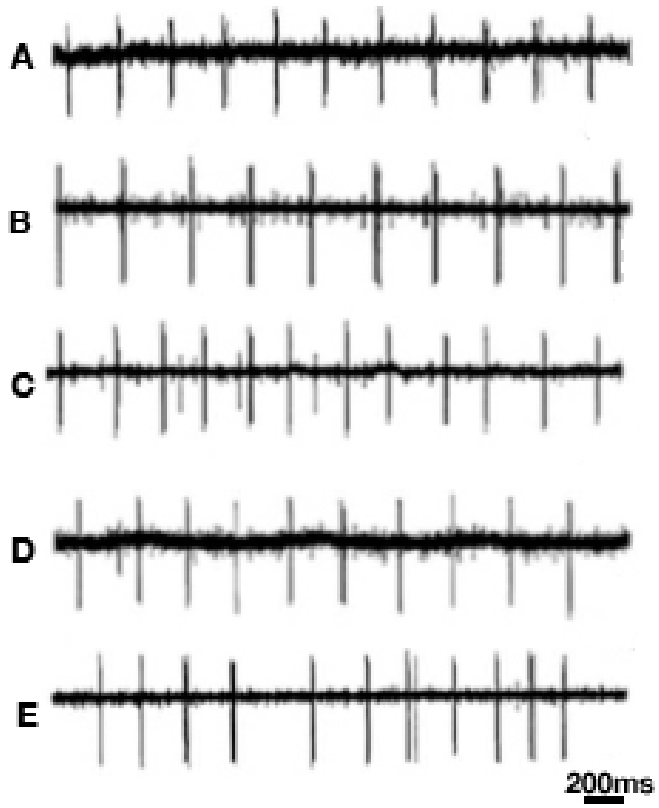

Figure 3.1: Extracellular recordings from the thalamus of patients suffering from different manifestations of TCD. All recordings were made in fully awake subjects during stereotactic neurosurgery. Each dash represents one LTS burst. A: Neurogenic Pain B: Parkinson's Disease C: Epilepsy D: Obsessive Compulsive Disorder and Major Depression E: Tinnitus. Data from [63].

A similar mechanism could be at work in patients suffering from tinnitus in which thalamic areas are deprived of auditory excitation due to the destruction of peripheral auditory tissue.

Parkinson's disease has been implicated with the progressive apoptosis of dopaminergic neurons. The consequence of this - mediated by the specific connectivity in the basal ganglia - is an overactivity of the globus pallidum that in turn inhibits motor areas in the thalamus. In this case, it is feasible that not hypoactivation but rather hyper-inhibition leads to the hyperpolarization of thalamic neurons.

Changes in EEG/MEG measures

In addition to the changes in the behavior of individual thalamic neurons researchers have noticed another peculiar difference between patients suffering from a thalamocortical dysrhythmia and healthy age-matched controls. When comparing the EEG and MEG measures of the two groups it became immediately apparent that the power spectra of patients are shifted upwards, indicating increased levels of synchrony [77, 110]. This increase in synchrony is particularly visible in the low alpha and theta frequency bands as well as in the beta-gamma bands (Figure 3.2). Important for the existence of a TCD-syndrome is hence a quantitative increase of low-frequency oscillations from the thalamus to the cortex.

Due to the time it takes a thalamic neuron to deinactivate a sufficient number of calcium channels to emit a burst, there is a minimum interburst interval of roughly 200 ms [75]. This interval corresponds well with the observed shifts in frequency. Furthermore, it is known from research done on sleep oscillations that thalamic bursts are very well suited to synchronize large ensembles of neurons. Indeed, when looking at the coherence between extracellular thalamic recordings and EEG measures in patients, Sarnthein et al. [110] found that there is strong coupling between the thalamic and cortical signal, as well as a constant phase relationship (Figure 3.3). This data corroborates the hypothesis that thalamic changes are responsible in producing the large-scale measure changes in EEG/MEG.

3.1.2 Persistence

When looking at the changes described in Section 3.1.1 one thing becomes especially apparent. If thalamic bursting is to influence large-scale synchrony as measured by EEG or MEG techniques two factors need to interact in synergy.

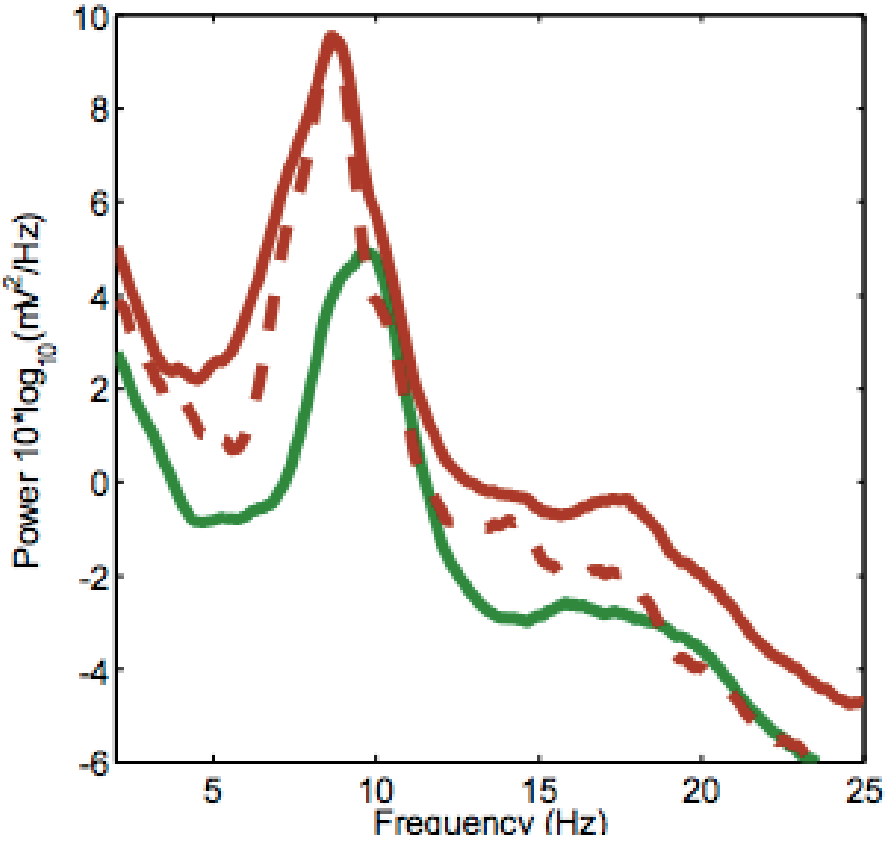

Figure 3.2: Averaged EEG power measures of patients (red, N=17) versus healthy controls (green, N=15). Higher levels of synchrony can be found especially in the theta and gamma bands coupled with an overall low-frequency shift. The dashed red line demarks the patient group averaged without accompanying medication. From [111].

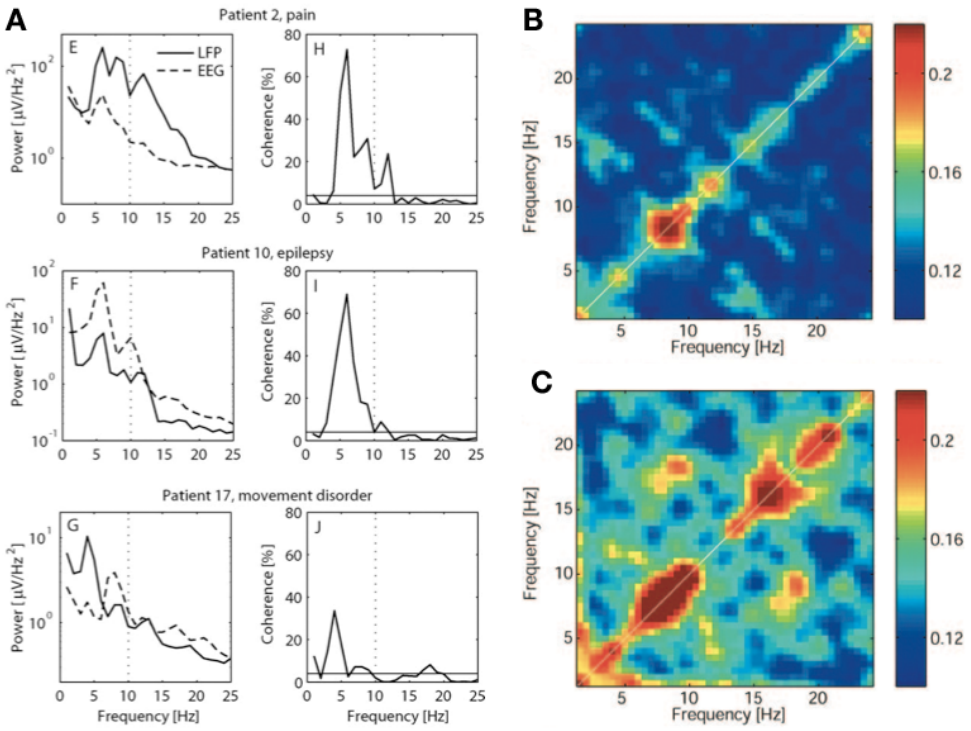

Figure 3.3: (A) Coherence and bicoherence measures comparing (B) healthy age-matched controls with (C) patients. (A) Shows power spectra and coherence measures for patients suffering from different TCD manifestations. The right column shows the coherence over frequency between the LFP and EEG measures (solid line marks significance). In (C) bicoherence peaks are apparent in the theta-theta beta-beta and theta-beta domains in the patient group but to a lesser extend in the control group (B) [110].

Firstly, thalamic neurons need to synchronize over extended areas of tissue. As discussed above bursts are salient events that can lead to synchronous activity in postsynaptic neurons. It is therefore feasible that an increase in the burst incidence concomitantly leads to an increase in synchrony.

Secondly, there also need to be rhythmic oscillations in order to drive thalamic and cortical neurons persistently. Indeed, Jeanmonod and colleagues found a large number of neurons that were bursting rhythmically with a very high reliability (see Figure 3.1) when recording extracellulary [65]. This rhythmicity is paramount in persistently driving cortical neuron ensembles to exhibit the shifts in EEG measurements. The observed pattern points to about one quarter of the

recorded neurons being engaged in a rhythmically bursting regime. Another quarter is bursting arrhythmically, and the rest is firing sporadically [63].

Here we want to answer the question of how these particular physiological characteristics are produced in TCD. We furthermore want to shed light on which mechanisms are feasible contenders for the generation of bursting as well as low-frequency rhythmic oscillations. In the following section we outline some possible mechanisms for the generation of rhythmic and persistent bursting in the thalamus.

3.2 Mechanisms

The mechanisms described in the following can roughly be subdivided into cell-intrinsic and network mechanisms. I try to discuss each separately, even though it is feasible, or even likely, that these mechanisms are not mutually exclusive and interactions might occur.

3.2.1 Sporadic excitation

The simplest scenario is sporadic excitation from sources outside the affected thalamocortical module. During wakefulness it is feasible that overall excitation is interacting with a hyperpolarized thalamic neuron to intermittently trigger LTS bursts. These sporadic excitations would have to be of a large amplitude in order to depolarize the thalamic neuron sufficiently for burst generation. The resulting pattern would be sporadic bursting in TCD-affected thalamic areas with inter-burst intervals according to the burst refractory period of the cells (ca 200 ms). In a single column model this mechanism does not lead to regular oscillations. However, if individual bursting neurons are embedded in a network of connected neurons, synchronous burst discharges might occur. Note, that only about a quarter of the identified thalamic neurons burst regularly. This mechanism is therefore a very likely candidate for the generation of irregular bursts.

3.2.2 Pacemaker current

The second scenario is based on cell-intrinsic mechanisms. It has been shown ([56, 87], etc.) that many thalamic relay cells host hyperpolarization activated cation channels, so-called h-channels. These channels have also been found in other organs than the brain and are known to act in pace-maker cells in structures engaged in constant oscillations. This h-current in the thalamus is modulated by

cell-intrinsic calcium levels. After the massive calcium influx of an LTS burst the h-current will be very low, not interfering with the subsequent hyperpolarization. This hyperpolarization will then slowly activate cation influx and hence depolarize the cell until it reaches bursting threshold and emits another LTS burst. In fact, it has been observed in vitro that cat LGN thalamic neurons engage in repeated oscillations in the 2-4Hz range [86]. These properties make the h-current an ideal driver of hyperpolarization triggered pathological oscillations in thalamocortical dysrhythmia.

3.2.3 RTN feedback loop

Delayed inhibitory feedback is the source of all oscillatory mechanisms. This feedback can occur intrinsic to the neuron, as in the example discussed above or by extrinsic network factors. Two possible feedback loops can provide the necessary negative feedback in a thalamocortical module: The RTN feedback loop consists of thalamic relay nuclei that are reciprocally connected with the GABAergic neurons in the thalamic reticular nucleus. Relay excitation hence leads to a delayed negative feedback. If that feedback is strong enough, it is possible that the thalamic relay neurons get hyperpolarized for a significant period of time leading to a progressive deinactivation of inherent t-type calcium channels [75]. When the inhibitory input from the RTN ceases, the relay neurons will be released from hyperpolarization and will likely be able to emit a low-threshold spike burst. Bursting in the thalamic relay nuclei has a dual effect on the thalamic reticular nucleus. Firstly, bursts provide very prominent excitation as several action potentials follow each other within a short interval. Secondly, the bursting in the relay nuclei will also prevent runaway spiking during the relatively long refractory period following a burst. This leads to a high signal to noise ratio of excitation in the thalamic reticular nucleus. Earlier models have suggested that burst generation in the thalamus is favoured by powerful afferent excitation under relatively low-activity background conditions [38]. Therefore, within this feedback loop there is an inherent tendency to start burst generation if this is not actively prevented by tonic excitation.

3.2.4 Cortical feedback loop

There also exists a 'long' feedback line via cortical layer VI neurons which project back to afferent areas in the thalamus, in particular to the thalamic reticular nucleus. This can have a dual effect on thalamic neurons. On the one hand there is direct excitation from the corticothalamic fibers, and on the other hand

there is indirect inhibition from corticoreticulothalamic connections. The latter has been hypothesized to be very prominent under some conditions and is favored by the size and location of cortical synapses on reticular neurons [68].

In order to validate and contrast the candidate mechanisms described above we have developed a computer model of a single thalamocortical loop consisting of thalamic relay and reticular cells as well as a cortical component (Figure 3.4). As discussed above, oscillation is a consequence of feedback loops and several of these are implemented in this thalamocortical system. These can occur on the sub-cellular level, implemented by ion channels on the cell membrane of individual neurons, as well as through the interconnectivity between neurons, either by excitation or inhibition.

3.3 Methods

3.3.1 Model architecture

The present model consists of 3 model neurons - a thalamic relay neuron, a thalamic reticular neuron and a cortical neuron. We assume that individual action potentials from each of these cells can drive their counterparts in the other areas. The thalamic relay cell has excitatory connections to the reticular and cortical model component. Note, that these represent the main afferent input of information to the cortex. The thalamic reticular neuron receives excitatory input from the cortex and thalamic relay and directly inhibits the thalamic relay (see Figure 3.4). The cortical component has random excitatory corticocortical afferents as well as receiving excitation from the underlying thalamic neuron. It in turn excites the thalamic reticular and relay neurons.

Each neuron is modeled by integrate-and-fire dynamics. In the case of the thalamic cells t-type calcium currents as well as h-currents are added to the passive leak current [117]. Thalamic afferent input is modeled by Poissonian excitatory spike trains.

3.3.2 Neuron model

In this model we employ the integrate-and-fire-or-burst cells proposed by Smith et al. [117]. We do so to reduce the amount of free parameters as well as speed

up simulations. The neuron is described by the following equations that extend a classical conductance-based leaky integrate-and-fire neuron by the slow t-current I_T. We also include a representation of the hyperpolarization-activated cation current I_H.

$$C\frac{dV}{dt} = I_{inp} - I_L - I_T - I_H \tag{3.1}$$

where I_{inp} corresponds to the combined synaptic current and I_L is the leak current. The t-current is then described by the following equation.

$$I_T = g_T m_\infty h(V - E_T) \tag{3.2}$$

Its dynamics are described by the activation m and the deactivation h. Whereas m is instantaneously activated by means of

$$m_\infty = H(V - E_h) \tag{3.3}$$

with H being the heaviside step function, we model h explicitly with

$$\frac{dh}{dt} = \begin{cases} -h/\tau_{h1} & \text{if } V \geq E_h, \\ (1-h)/\tau_{h2} & \text{if } V < E_h. \end{cases} \tag{3.4}$$

Here, if the membrane potential V is above the deinactivation threshold, h decreases with timescale τ_{h1}. If, on the other hand, the membrane potential falls below this threshold, deinactivation tends to 1 with timescale τ_{h2}. Functionally, τ_{h1} determines the length of the bursts, whereas τ_{h2} is responsible for the time it takes a thalamic neuron to deinactivate enough calcium channels to burst upon release from the hyperpolarization. In the next timestep the membrane potential is then reset to V_{reset}.

The leak current I_L is simply

$$I_L = g_L(V - E_L) \tag{3.5}$$

Spiking dynamics are implemented by making the sodium spike instantaneous whenever the neuron's membrane potential crosses the spiking threshold V_θ.

In order to capture the dynamics of the low-voltage activated calcium-dependent cation current I_H we need to explicitely derive a description of the intracellular calcium level $[Ca^{2+}]$, which in turn is dependent on the magnitude of the t-type calcium current I_T. We model $[Ca^{2+}]$ with

$$\frac{d[Ca^{2+}]}{dt} = -\alpha I_T(1 - [Ca^{2+}]) - \beta[Ca^{2+}] \tag{3.6}$$

α and β are the calcium accumulation and decay parameters, respectively. I_H is then a function of the intracellular calcium levels as well as the activation function m_H.

$$I_H = g_H m_H(V)(1 - [Ca^{2+}]) \tag{3.7}$$

with

$$m_H(V) = 1/(1 + exp((V + 75)/5.5)) \tag{3.8}$$

The after-hyperpolarization following a burst of action potentials leads to an activation of I_H that, due to its slow time course depolarizes the neuron with enough t-type calcium channels deinactivating to trigger another burst. Over many cycles the intracellular calcium accumulates and counteracts this pace-making mechanism. This has been hypothesized to be the source of the waxing-and-waning envelope of so-called sleep spindles that occur at the transition between slow-wave sleep and wakefulness [126, 34].

In the following I contrast the three different feedback mechanisms that might explain the rhythmic and persistent burst generation in thalamocortical dysrhythmia. I change critical parameters to gain an estimation of how feasible each mechanism is with reference to parameters estimated by in vivo and in vitro studies.

3.4 Results

3.4.1 Intrinsic bursting

Intrinsic bursting relies on feedback mechanisms intrinsic to the neuron. As outlined above this role can be played by a low-voltage activated cation current I_H that is activated during the burst after-hyperpolarization and leads the neuron back to the t-type calcium channel activation threshold.

This mechanism has been shown to be responsible for rhythmic processes in different organs. A similar ion-channel has for example been identified in heart muscles, where it can play a role in the control of the heart beat [4], or in the respiratory system of mammals[28].

In the intrinsic bursting scenario, all neurons are self-sufficient and the whole thalamocortical module is driven by the thalamic relay neurons. Weak coupling

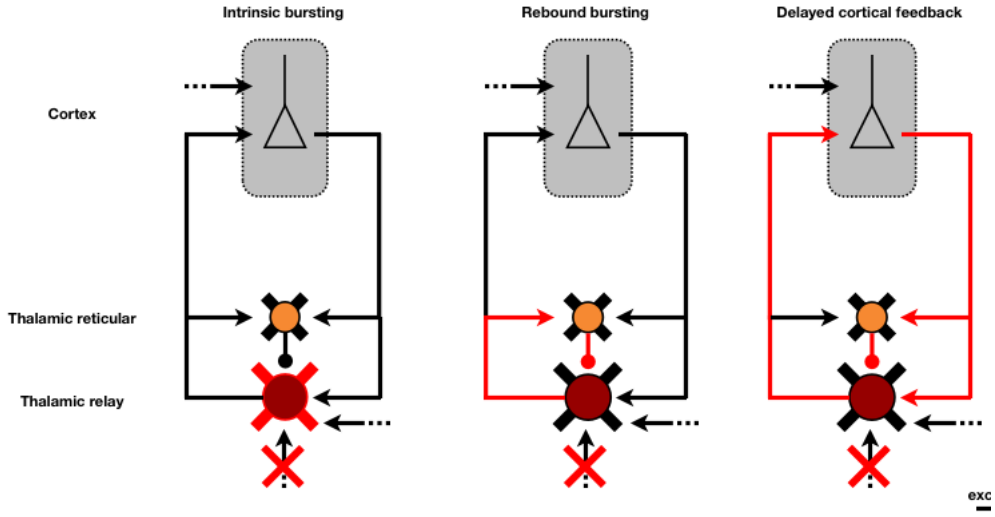

Figure 3.4: Feedback circuits in a model of a thalamocortical module consisting of thalamic relay, thalamic reticular nucleus and cortex. Sharp arrows denote excitatory, round arrows inhibitory connections. The common manipulation of all data presented here is the deafferentation of thalamic afferent fibers. Dotted arrows are excitatory Poissonian input. The three relevant hypotheses are marked in red.

among thalamic relay neurons might lead to the synchronization of large ensembles and hence to the development of the dysrhythmia. The frequency of bursting will then be highly-dependent on the conductance of I_H. Figure 3.5 (top) shows how an increased conductance leads to higher burst frequencies. This, of course, is limited by the t-type calcium channel mediated relative refractory period which limits the frequency to roughly 4 Hz in this model. Another characteristic of the current model is that the higher the bursting frequency, the lower the amount of spikes in the burst (Figure 3.5, bottom).

A comparison of voltage traces from cat in vivo recordings [86] versus the current model is shown in Figure 3.6. Our neuron model by Smith et al. [117] with the h-current modifications approximates the behaviour of thalamic neurons reasonably well. This is also the case if the neurons are embedded in the model of a typical thalamocortical circuit. The strength of feedback connections in this setting can be set to be arbitrarily small as external feedback is not necessary to drive the system. To the contrary, any kind of external manipulation has a strong negative influence on the regularity of bursting the thalamic relay neurons. This is shown in Figure 3.7. Even small amounts of noise can make the neuron fire less regularly. This is due to the relatively low conduc-

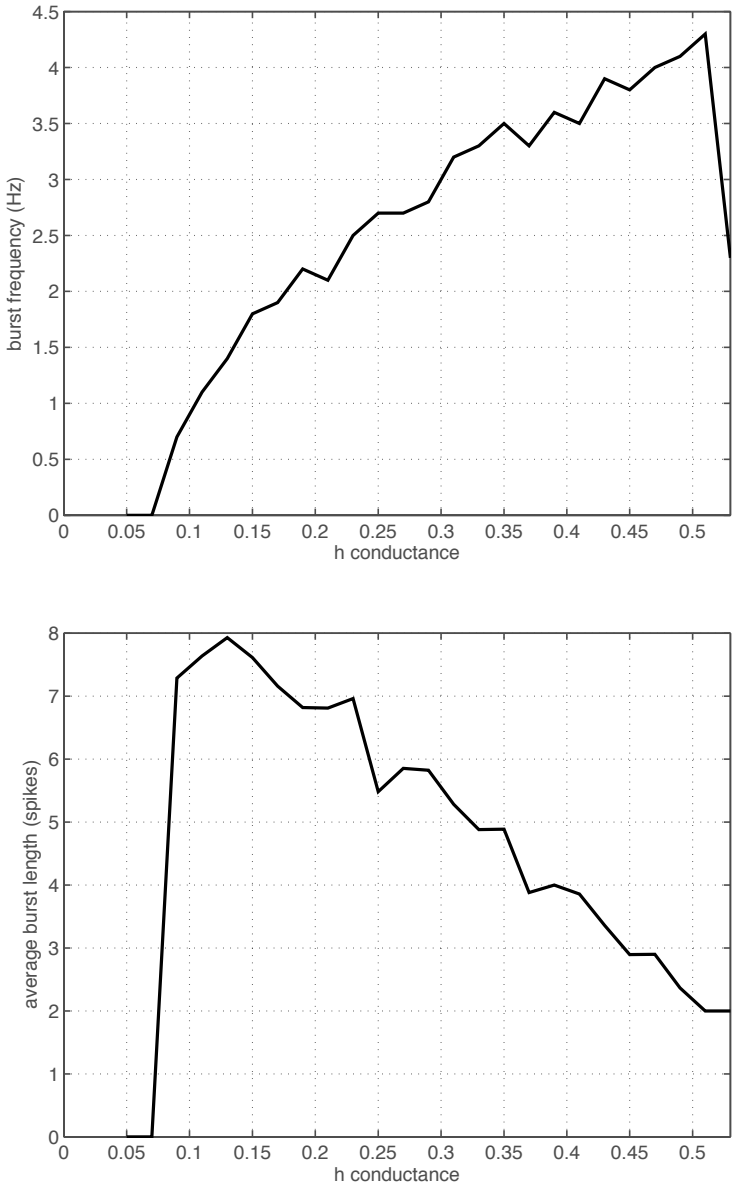

Figure 3.5: The effect of H-conductance on bursting behavior. Top: Higher conductances lead to quicker depolarization in between bursts. The curve breaks off at 4Hz because the time between bursts becomes to small to deinactivate t-channels. The noise stems from numerical inaccuracies and missed bursts with the burst-finding algorithm. Bottom: H-conductance versus the average number of spikes in a burst. With increasing frequency the number of spikes in a burst decreases drastically, because less t-channels can get deinactivated.

tivity mediated by the h-current. If an input spike excites the thalamic neuron during its relative refractory period, this can lead to a significant increase in the interburst intervals, because it will take more time for enough t-channels to deinactivate to generate the next burst. We investigated this systematically in Figure 3.8. The autocorrelogram shows strong rhythmicity with low levels of Poisson noise, which then deteriorates the more spikes are fed into the system.

3.4.2 Rebound bursting

The short feedback loop via the reticular nucleus is well-known to play an important role in the generation of slow-wave sleep rhythms [35]. Reticular neurons have a strong inhibitory influence on thalamic relay neurons and can potentially recruit rebound bursts. In this setup we have switched off the h-current investigated in Section 3.4.1 so the behavior observed is based exclusively on network effects. Timing plays an important role in driving this oscillation. Within the interplay of reticular and relay neurons it is imperative that excitation and inhibition occur at the right points in time. Otherwise, the two neurons will not be able to recruit each other. There are two possible ways in which this might be achieved. Firstly, the connections between areas could yield a delay that is consistent with the relative refractory periods of the bursting relay neurons. However, connection delays within the thalamus are generally assumed to be short, and in no way approaching the 200 ms necessary. The other candidate mechanism, the one implemented in this model, is a delay mediated by the time-constants of the inhibitory synapses of reticular neurons on relay neurons. If the inhibition from reticular neurons is strong enough and decays slowly enough the relay neuron will be hyperpolarized for a sufficient amount of time to emit a burst upon release of the inhibition. This mechanism is shown in Figure 3.9.

The time course of the reticular inhibition in combination with synaptic efficacy thus plays an important role in determining the rhythmicity of the system. This is shown in Figure 3.10. Autocorrelations yield relatively weak rhythmic behavior and this only with strong inhibition and long synaptic time constants (black line). This rhythmicity decays when either the synaptic time-constant (red line) or the synaptic efficacy are decreased.

A different picture emerges if the reticular neurons themselves are in bursting mode, which could be caused by a change in the input statistics to these neurons. A lack of activation due to deafferentation or overinhibition of relay neurons could lead to a subsequent reticular hyperpolarization. If a hyperpolarized reticular neuron receives excitation from a relay neuron it will in turn emit a burst of action potentials, that contributes to the conditions of rebound

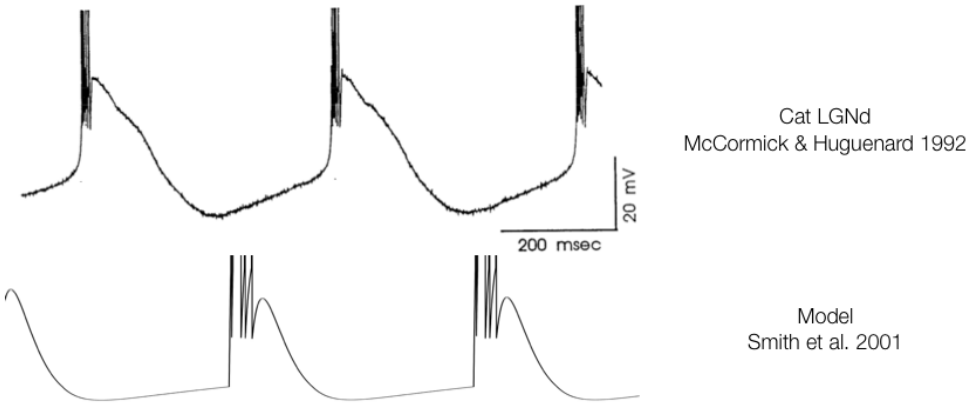

Figure 3.6: Example voltage traces of cat in vivo recordings from bursting thalamic neurons [86] versus the current model. Burst frequency, length, and shape are well-approximated by the current equations.

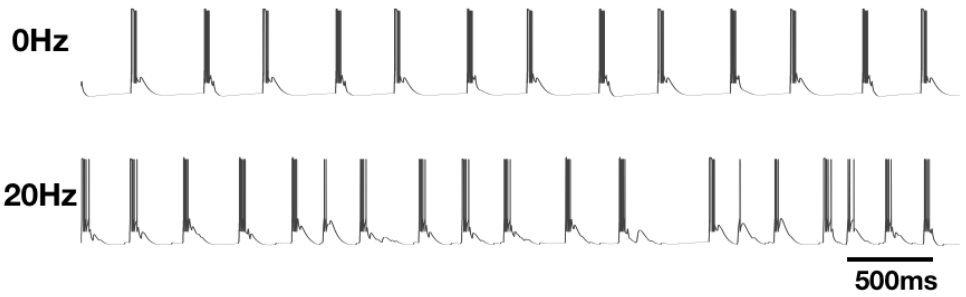

Figure 3.7: Voltage traces from the thalamic relay component of the circuit under dysrythmic conditions. Top: Trace at 0Hz noise conditions. Bottom: Excitatory Poissonian noise at 20 spikes per second disturbs the intrinsic rhythm of the neuron.

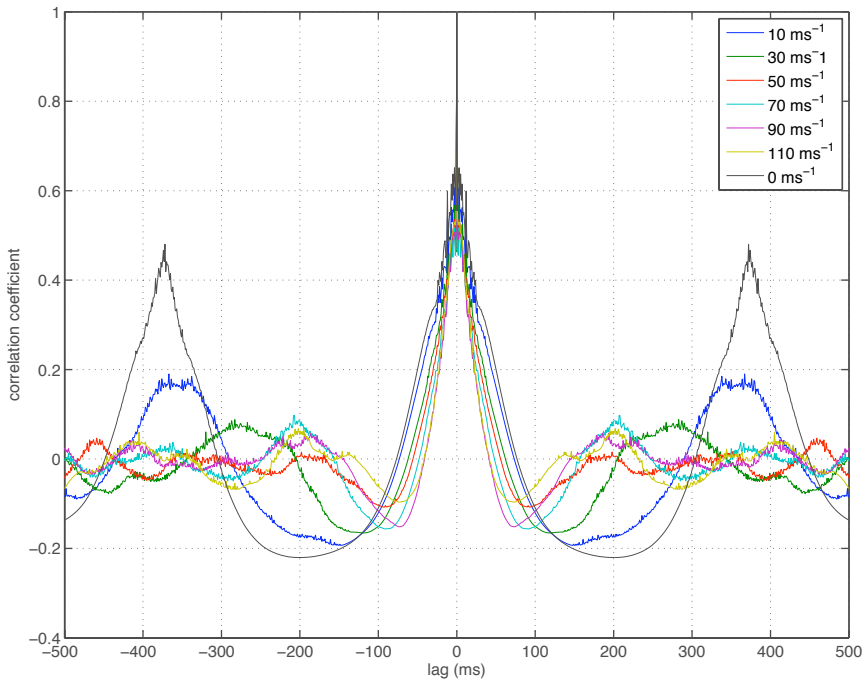

Figure 3.8: The effect of noise on rhythmicity in h-current pacemaker cells. The h-current is very fragile with respect to noise as is apparent from the autocorrelation of the membrane potential. Under no-noise conditions there is regular bursting at 3 Hz. This speeds up but becomes less regular under noisy conditions (poissonian noise).

oscillations stated above: a burst of action potentials will have a higher efficacy as well as a longer time-constant than an individual spike.

This is shown in the autocorrelations in Figure 3.10 (right). The larger amount of afferent spikes also interacts with the synaptic time constant. In general, it is apparent that the longer the synaptic time-constant the more rhythmic the oscillation. Also, the longer the time-constant the slower the oscillation frequency.

3.4.3 Delayed cortical feedback

The delayed cortical feedback mechanism, similar to the mechanism described in Section 3.4.2, relies on well timed cortical feedback to reinitiate oscillation

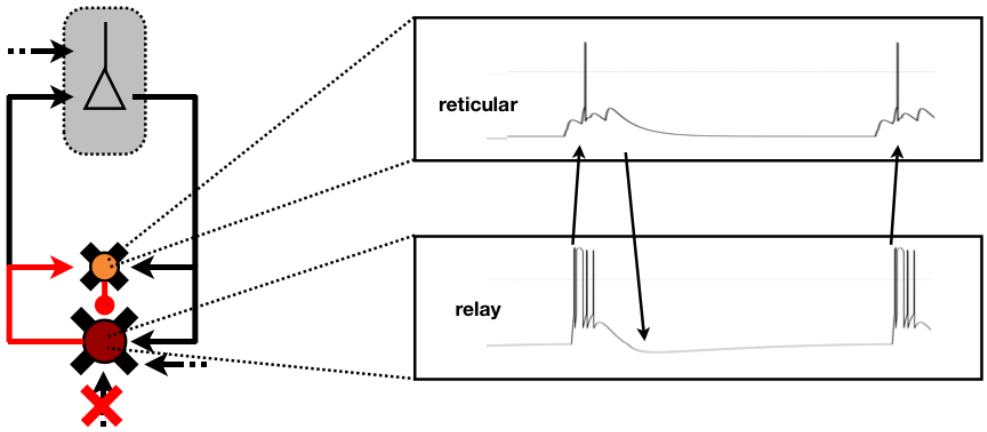

Figure 3.9: Schematic of the short feedback loop leading to rebound bursts between thalamic relay and thalamic reticular nuclei (marked in red). Shown are voltage traces of reticular (top) and relay (bottom) neurons. Arrows indicate consecutive events in the rebound bursting mechanism.

cycles.

Cortical rebound excitation can only reinitiate a cycle if the excitation hits the hyperpolarized thalamic neuron after its relative refractory period. Thus, there needs to be a delay of on the order of 150 ms for the excitation to complete the circuit loop. This is shown systematically in Figure 3.11.

There is a sharp difference in the models behavior between delay times of 120 and 150 ms. The effect that these delays have on the thalamic relay neuron are exhibited in Figure 3.12. If the delay of reexcitation is 120ms (upper trace) the excitation reaches the thalamic neuron during its relative refractory period and a new cycle will not be initiated. If on the other hand the delay is 150 ms enough t-type calcium channels have deinactivated after the previous burst to allow the initiation of another cycle. Obviously, the longer the delay the slower the oscillation frequency (Figure 3.11).

3.5 Discussion

In this chapter I have shown a simple model of burst generation in the thalamus in response to deafferentation of thalamic relay neurons. I have contrasted three different mechanisms for the production of regular and persistent 4 Hz bursting. In addition, I have discussed sporadic excitation as a valid mechanism for the

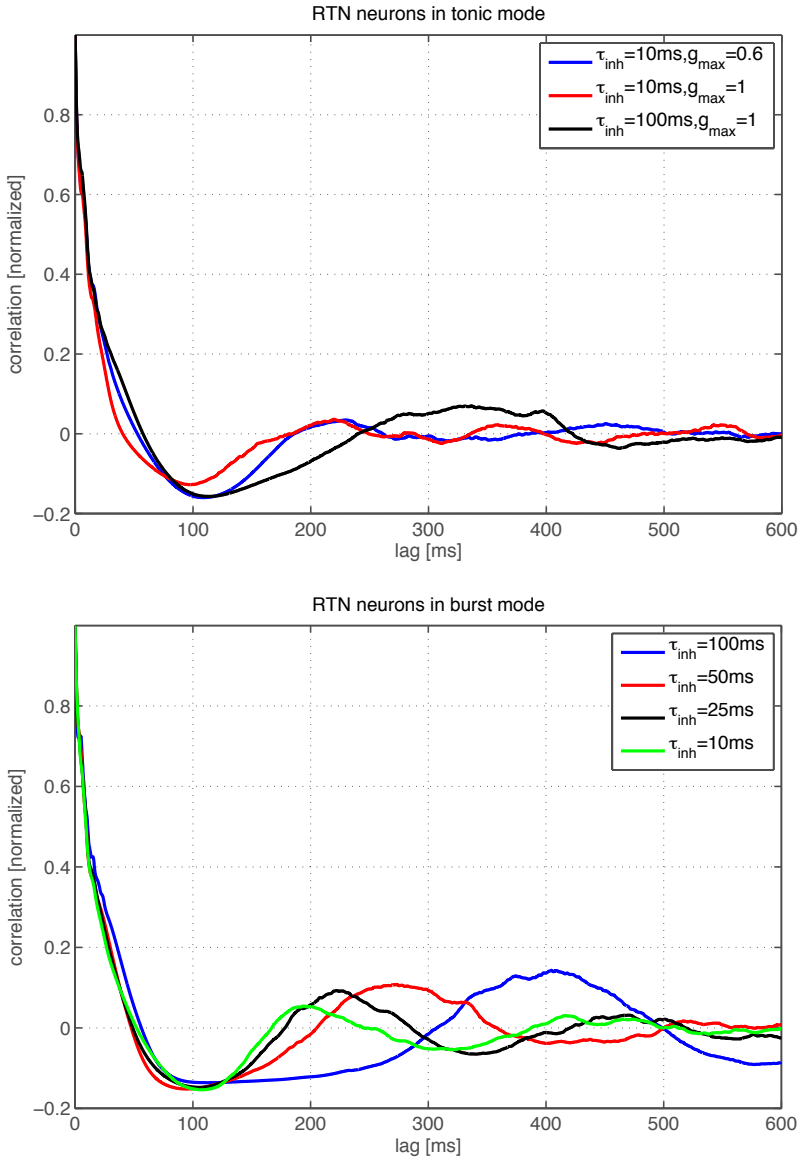

Figure 3.10: Comparison between rebound bursting mechanism with tonic (left) and bursting (right) thalamic reticular neurons.

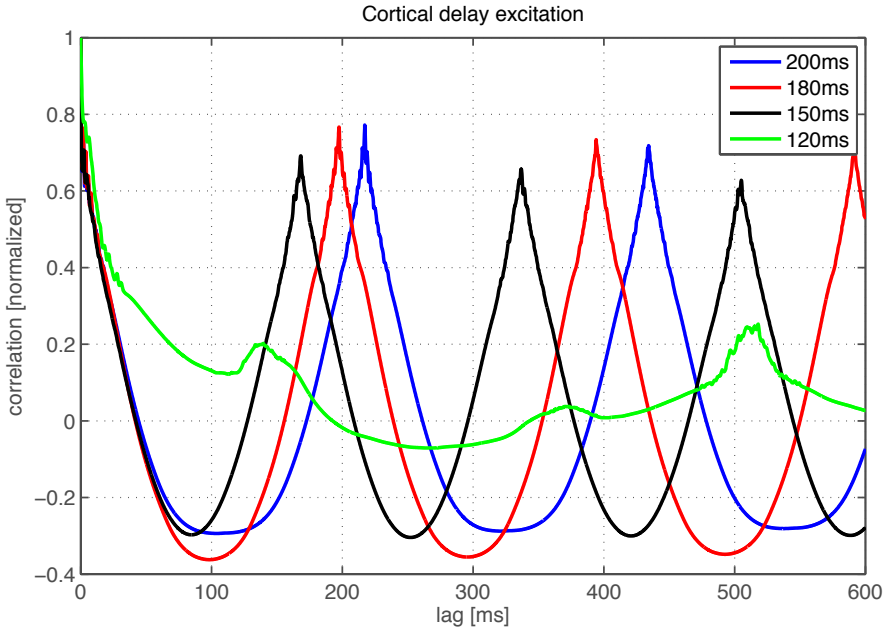

Figure 3.11: Autocorrelation of thalamic relay activity at different cortical delay times. Note the difference between 120 ms delay (green) and 150 ms delay (black) curves.

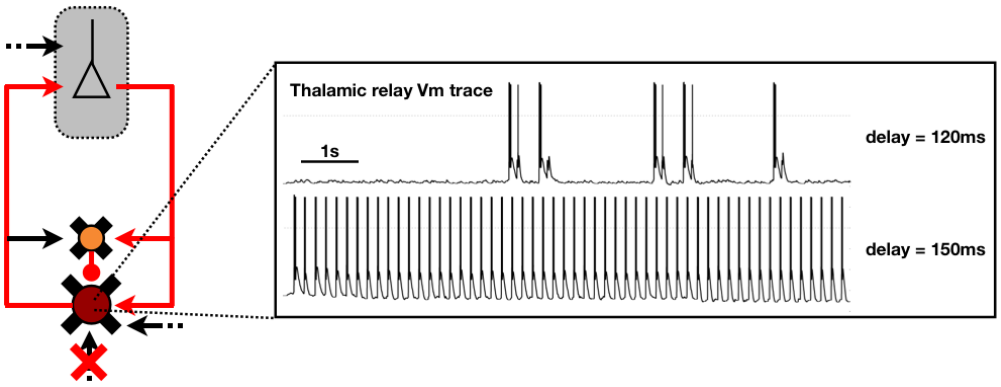

Figure 3.12: Schematic of the delayed cortical feedback mechanism (outlined by red connections). On the right are example traces from the thalamic neuron at different delay inputs.

generation of irregular bursting.

The frequency of the bursting observed in this model is mainly a product of cell-intrinsic processes. Enough t-type calcium channels need to deinactivate in order for a new burst to be initiated. All mechanisms described in this chapter interact with the relative refractory period of the thalamic relay neurons to some extent.

3.5.1 Intrinsic bursting

The intrinsic bursting mechanism relies on a specific current that cell-intrinsically depolarizes thalamic neurons after a burst has occurred. The neuron is setup to be hyperpolarized after the emission of the burst. This leads to a direct deinactivation of t-channels after a burst. The h-current is then responsible for the neuron to reach a membrane potential level at which the t-channels can activate and carry the next burst. The maximal conductance of the h-current determines the interburst interval. However, if the conductance is too strong there will not be enough time for t-channels to deinactivate and hence there will not be a burst upon reaching the activation threshold.

There is ample evidence for the existence of an h-current in thalamic relay neurons [56, 87, 98]. The intrinsic bursting has been observed under conditions in the cat LGN in the absence of external stimulation and is assumed to exist in other thalamic nuclei as well. The conditions provided during the deafferentation leading up to a thalamocortical dysrhythmia are hence ideally suited to provoke the intrinsic bursting mechanism. The downside, as was shown in Section 3.4.1 is the sensitivity of this mechanism to noisy conditions. Because of the relatively low strength of the h-current in comparison to external influences there is a strong tendency of the thalamic relay neuron's bursting to become arhythmic. For this reason, it is likely that the h-current mechanism of persistent and rhythmic bursting is supplemented by another mechanism that is more stable in noisy conditions.

3.5.2 Rebound bursting

The rebound bursting mechanism is based on the slow release from inhibition provided by long inhibitory synaptic time constants from reticular neurons to thalamic relay neurons. While conduction delays between thalamic nuclei are supposed to be relatively short (on the order of a few milliseconds) the long time-constants of GABA receptor-mediated inhibition are suited to grant a sufficient deinactivation of t-channels between bursts. Furthermore, this mechanism

is more robust to noise than intrinsic bursting as it relies on network feedback.

Rebound bursting as described above has been hypothesized to play an important role in the dynamics of slow-wave sleep rhythms [35, 118]. During the onset of sleep, changes in the resting membrane potentials of thalamic neurons are assumed to change, mediated by neuromodulatory input from extra-thalamic sources [37]. It is feasible that such mechanisms are akin to the change in membrane potential caused by chronic deafferentation or overinhibition of thalamic relay neurons. In such a framework, TCD-affected areas could be said to be asleep, with the important difference that sleep here is local compared to the large-scale oscillations observed during physiological sleep and states of deep anesthesia in vivo.

One prediction made possible by the current model is that reticular thalamic neurons are engaged in bursting activity as well as the thalamic relay neurons, which is also consistent with the sleep analogy [35]. Here we have shown that oscillations under conditions in which both thalamic relay and reticular neurons are in burst mode enable a much wider range of possible parameters for stable bursting oscillations. The reticular bursts then have a dual beneficial effect in recruiting bursts in thalamic relay neurons as compared to single reticular spikes. Both the amplitude and the time course of the resulting inhibitory post-synaptic potential make the occurrence of rebound bursts more likely.

3.5.3 Delayed cortical feedback

In our model, the delayed cortical feedback mechanism works only at very long delay periods. Thalamocortical conduction delays are supposed to be much shorter than the required 150 ms to allow for the recruitment of bursts in response to recurrent cortical excitation measured here. Hence, for this mechanism to work some sort of internal cortical delay would be necessary. At present, it is not clear how this could be implemented. Furthermore, the main recurrent feedback is generally supposed to be mono-synaptic via layer VI corticothalamic neurons.

This of course is not to say that the cortical influence can not have an important synchronizing effect on the thalamic modules generating the low-frequency oscillations. The importance of corticothalamic feedback in the synchronization of sleep rhythms has also been shown in vivo [8, 12, 25].

The anatomy of a thalamocortical module as presented in this model also allows for another feedback loop via the corticoreticular connections. By this, the cortex can have an indirect inhibitory effect on the thalamic relay neurons. It is possible that the rebound mechanism discussed above is in fact mediated via

these indirect connections. It has been shown that the corticoreticular synapses are larger and more proximal to the soma of reticular neurons than their thalamoreticular counterparts [68]. Furthermore, it has been hypothesized that the reticular neurons become sensitized to cortical inputs especially under sleep conditions [38]. This feedback loop would in principle have to obey the same conditions as the rebound burst mechanism above.

3.5.4 Synchronized sporadic bursting

The mechanism of synchronized sporadic bursting has not explicitly been investigated in this chapter as it entails the interaction between thalamocortical modules. However, it is a natural consequence of coupled networks of sporadically excited hyperpolarized thalamic neurons. In this scheme the lateral connections lead to a wave of burst discharges once one module is elicited to burst by random excitatory input. This leads to a chain reaction, that causes very strong excitatory post-synaptic potentials in the connected neurons. From the moment of one population burst discharge on, all neurons will have roughly synchronized refractory periods. Because many neurons are involved in this population oscillation the chances are high that one neuron within this population will receive sufficient input to burst shortly after the cessation of refractoriness. This will lead to a rhythmic oscillation with a period close to the burst-refractory period of the neurons. This works especially well in networks of dense connectivity.

3.5.5 Conclusion

A rebound burst mechanism in combination with h-current mediated intrinsic bursting seems to be the most viable mechanism for the generation of persistent rhythmic bursting in TCD. The rebound bursts can be generated equally well by intrathalamic pathways and thalamocorticothalamic connections.

Chapter 4

Low-frequency oscillations in thalamocortical circuitry

4.1 Introduction

The thalamus plays an important role in the generation of synchronous oscillations in the brain [1, 14, 27, 93]. The frequency of these oscillations has been shown to correlate well with states of vigilance [126]. For example, highly synchronous low-frequency oscillations can generally be associated with drowsiness and non-paradoxical sleep, whereas less synchrony is observed in the brains of awake animals [74].

The generation of these rhythms is based on the interaction of network anatomy with the specific physiological properties of thalamic neurons [39]. Recurrent connectivity between the thalamic relay and the thalamic reticular nucleus forms a delayed inhibitory feedback cycle that is the hallmark of all rhythmic oscillatory processes in the brain and other dynamical systems [43]. Thalamic neurons are endowed with ion-channels that allow them to engage in two different activation regimes [75, 86]. In the awake brain thalamic neurons are relatively depolarized and fire at rates proportional to their input currents. In contrast, under more hyperpolarized conditions, the same neurons are able to produce bursts of action potentials with intermittent periods of quiescence. T-type calcium channels that deinactivate in response to hyperpolarized membrane potentials are responsible for the generation of these bursts. Depolarization following prolonged hyperpolarization can activate the deinactivated channels and lead to the massive influx of calcium that is responsible for a slow large-amplitude depolarization. This depolarization can cause repeated sodium spikes that ride on the crest of the calcium spike. This behvior has been termed a low-threshold (LTS) calcium burst.

Thalamic neurons in both the relay nuclei and the reticular nucleus show increased incidence of calcium bursts during high-synchrony states such as non-paradoxical sleep [16, 91, 124]. The biophysical properties of these neurons then interact with the network connectivity to engage hyperpolarized thalamic relay and reticular neurons in a cyclical activation regime. Relay bursts are ideally suited to drive reticular bursts that in turn recruit new relay bursts by evoking strong inhibitory post-synaptic potentials (IPSPs) [133, 123, 34]. It has been hypothesized that this mechanism serves to limit the amount of information throughput to the neocortex during sleep states, by rhythmically inhibiting thalamic relay neurons [126].

Bursts are a ubiquitous phenomenon in the healthy brain. However, there is ample evidence that local production of low-frequency high-synchrony oscillations is central to a number of functional brain disorders combined under the name of thalamocortical dysrhythmia (TCD) syndrome [63, 77, 76, 65]. Sudden

changes in the input to thalamic circuits either from subcortical areas below or cortical areas above can switch the activation mode of thalamic neurons from tonic spiking to low-frequency bursting, even in the awake brain. These oscillations can spread by means of divergent connections in intrathalamic and thalamocorticothalamic circuits to produce significant shifts in patients' EEG and MEG recordings [77, 112, 111, 129, 89]. Furthermore, low-frequency oscillations can tip the balance between cortical excitatory-inhibitory networks and produce a persistent increase in cortical activation leading to the generation of positive symptoms [78, 77]. The manifestation of symptoms then depends exclusively on which modality-specific subsystem of the brain is affected by the dysrhythmia. TCD has been shown in somatosensory, motor, and auditory domains leading to neuropathic pain, Parkinsonism, and tinnitus, respectively. Furthermore, there is evidence for similar mechanisms affecting associative domains leading to neuropsychiatric disorders such as major depression, obsessive-compulsive disorder, and schizophrenia [76, 89, 111, 129]. Similarly, some forms of epilepsy can be indicative of a thalamocortical dysrhythmia syndrome [63, 109].

TCD in the somatosensory domain leads to chronic neurogenic or neuropathic pain. This depends on the following sequence of events [77]: Peripheral damage to nerve fibers leads to a lack of excitation in both the ventro-posterior areas of the thalamus as well as in parts of the multimodal intralaminar nuclei (in particular the posterior region of the central-lateral nucleus of the thalamus - pCL). The resulting attenuation of excitatory input switches individual thalamocortical circuits from high-frequency tonic firing to a low-frequency bursting regime. This is corroborated by findings of increased bursting incidence in the CL of TCD patients [71, 63, 62, 83]. Furthermore, the local field potential (LFP) in the thalamus is highly coherent with the low-frequency shift in the EEG recordings [109, 89, 111, 129] and typically is spatially consistent with the observed symptoms. This indicates that there is synchronization between affected thalamocortical circuits. It is also likely that affected circuits are able to recruit progressively more and more circuits into the low-frequency regime by means of divergent connections at the intrathalamic, corticothalamic, and thalamocortical level. In accordance with the proposed source of TCD, neurosurgical removal of the parts of the thalamus most affected by the bursting alleviates symptoms significantly in the majority of patients suffering from therapy-resistant neuropathic pain [65, 66].

Due to the experimental intractability of the human thalamocortical system, there is an ongoing debate about the underlying mechanisms leading to functional neurological disorders associated with TCD. Here, we want to reproduce

TCD dynamics in a biologically constrained network model of the thalamus.

Specifically, we want to identify the conditions that lead to the onset and the maintenance of TCD. What are the mechanisms that lead from a change in thalamic afferent input to the persistent and rhythmic overproduction of low-frequency thalamocortical oscillations?

Furthermore, we want to investigate how anatomical changes to the thalamocortical circuitry can switch the system from a TCD state to a normal dynamical regime. By mimicking the process of functional neurosurgery in a computer model we aim to elucidate the mechanisms underlying the surgical control of pathologically increased slow TC oscillations.

Here, we make use of a large-scale computational network model of the thalamus to shed light on these open questions. We specifically model the somatosensory manifestation of symptoms in TCD in adhering to anatomical data from the ventral posterior (VPN) and central lateral (CL) system. However, the current results can be extended to incorporate all known domains of TCD.

4.2 Methods

4.2.1 Model architecture

The thalamic model consists of 3 independent groups each consisting of 100 neurons modeled as described above. The groups correspond to one specific relay nucleus (VPN), one non-specific relay nucleus (CL) and the thalamic reticular nucleus (RTN). These represent the three distinct nucleus types found in the thalamus. Here, we focus on the nuclei involved in somatosensory processing. But the same distinction between specific (SP) and non-specific (NSP) excitatory nuclei and inhibitory reticular nucleus holds true in other subsystems. Each group receives random excitatory stimulation modeled by a Poissonian spike train. The intrathalamic connectivity is characterized by the following principles. Firstly, the relay cells of the VPN and CL have excitatory connections with the RTN [94, 95, 48]. Reticular neurons in turn send back inhibitory connections to the relay nuclei [54, 127, 141]. We distinguish the first-order relay nucleus VPN from the intralaminar nucleus CL by implementing local one-to-one connectivity between VPN and RTN whereas connections between RTN and CL are characterized by divergent connections (see Figure 4.1A).

Synaptic connections are modeled by exponential decay functions and are triggered after a set delay time if the presynaptic cell reaches its firing threshold. The time-constant of decay is assumed to be faster for excitatory synapses than inhibitory synapses. Parameters are shown in Tabel 4.1.

Parameter	Value
Excitatory Synapse τ	10 ms
Inhibitory Synapse τ	30 ms
Delay VPN→RTN	3 ms
Delay CL→RTN	3 ms
Delay RTN→VPN	3 ms
Delay RTN→CL	3 ms

Table 4.1: Model parameters.

In order to keep the number of parameters manageable, we make a couple of simplifying assumptions. Axons in cortical layer VI not only project to the RTN but also send collaterals to the thalamic relay nuclei. In the present model we neglect these connections because thalamic low-frequency oscillations have been observed under conditions of cortical deafferentation [27]. Note that in the current model external excitatory input to thalamic relay neurons is not necessarily equivalent to peripheral excitation, but could represent top-down corticothalamic excitation as well.

Secondly, we model RTN without dendrodendritic gap junctions and intranuclear inhibition [30, 115, 141]. These connections have been shown to play an important role in the generation of spindle rhythms in the isolated reticular nucleus. Their role in complete thalamic circuits is less clear and we therefore neglect this type of connection.

It is generally assumed that interactions with neuromodulators can synchronize and desynchronize thalamic oscillations by manipulating the biophysical properties of individual cells [12]. We model these connections indirectly by changing input excitation explicitly (see description of neuron model below).

4.2.2 Neuron model

Thalamic neurons are modeled by the integrate-and-fire-or-burst model proposed by Smith et al. [117]. The neurons are described by the following equations that extend a classical conductance-based leaky integrate-and-fire neuron with a simplified model of the slow hyperpolarization-activated calcium current I_T.

The membrane potential of the neurons follows

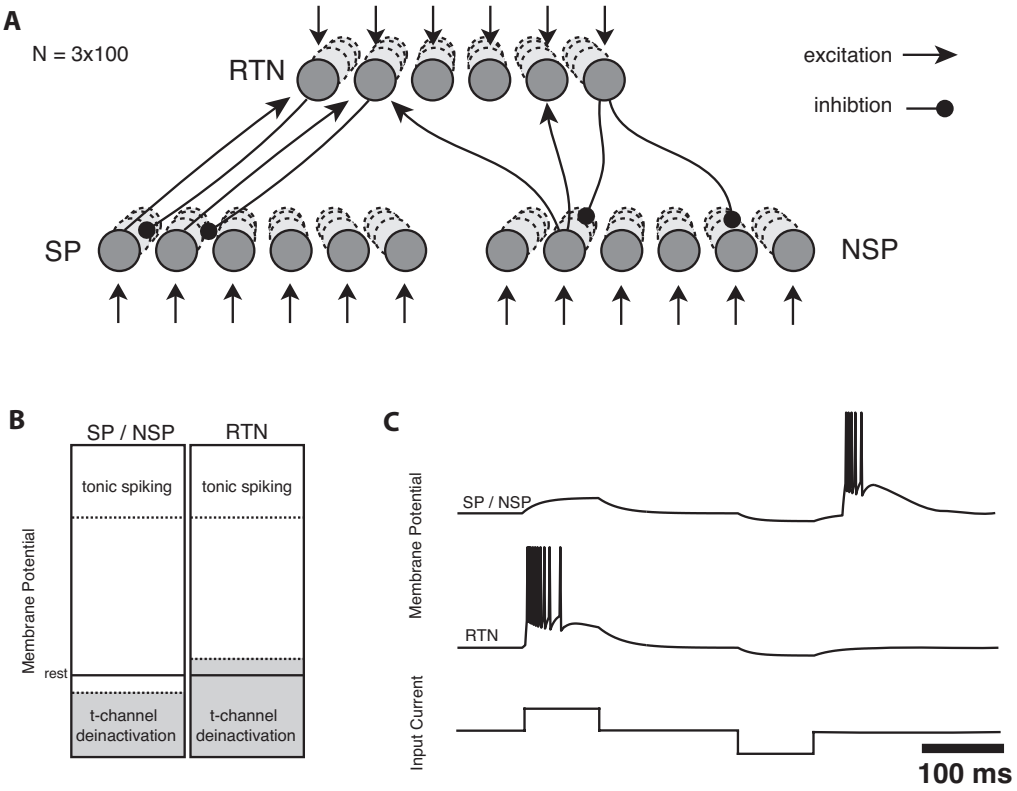

Figure 4.1: (A) Thalamic model layout. There are reciprocal connections between the relay and reticular parts of the model with SP-RTN connections following a one-to-one scheme and the NSP-RTN connections implementing some degree of divergence. (B) Shows the relationship of the physiologically relevant thresholds in the cell model and contrasts relay (SP/NSP) and reticular neurons. The t-channel deinactivation threshold lies below the neurons resting potential for relay neurons and above the resting potential for reticular neurons, leading to different bursting behaviors (C).

$$C\frac{dV}{dt} = I_{inp} - I_L - I_T \tag{4.1}$$

where I_{inp} corresponds to the combined synaptic current and I_L is the leak current which is simply

$$I_L = g_L(V - E_L) \tag{4.2}$$

The neuron produces a spike whenever the membrane potential crosses the threshold V_θ. On the timestep following the spike the membrane potential is then explicitly reset to V_{reset}.

The t-current is modeled by

$$I_T = g_T m_\infty h(V - E_T) \tag{4.3}$$

Its dynamics are subject to a two-stage deinactivation-activation cascade, described by the activation variable m and the deactivation variable h. Activation is assumed to occur instantaneously:

$$m_\infty = H(V - E_h) \tag{4.4}$$

with H being the heaviside step function. h is evolves slowly and is modeled by

$$\frac{dh}{dt} = \begin{cases} -h/\tau_{h1} & \text{if } V \geq E_h, \\ (1-h)/\tau_{h2} & \text{if } V < E_h. \end{cases} \tag{4.5}$$

If the membrane potential V is above the deinactivation threshold E_h, h decreases with timescale τ_{h1}. If, on the other hand, the membrane potential falls below this threshold, deinactivation tends to 1 with timescale τ_{h2}. Functionally, τ_{h1} determines the length of the bursts, whereas τ_{h2} determines the time it takes a thalamic neuron to deinactivate enough calcium channels to burst. As described by Equation 4.4 activation of the t-channels and the triggering of the calcium burst occurs instantaneously upon depolarization across the threshold E_h.

The behavior of this model neuron can be understood largely in terms of the the resting potential E_L in relation to the t-channel activation/deinactivation threshold, E_h (Figure 4.1B). If the membrane potential is below E_h t-channels progressively deinactivate. For a burst to occur the neuron needs to be depolarized to the threshold and upon crossing of E_h the activation gets triggered.

Generally, thalamic relay and reticular neurons are both endowed with the same calcium spike producing mechanism. However, physiological and morphological studies have lead to the discovery of a number of important differences. These manifest in particular in the timescales of inactivation of the t-type calcium channels, which is generally slower in RE neurons [35, 134]. Furthermore, recent detailed modeling studies of these types of neurons have shown important differences in which afferent stimuli are able to trigger bursts in RE and TC neurons [38]. This is based on the location of both the t-channels as well as the excitatory and inhibitory synapses from different sources [72, 73]. We try to capture these results in a simplified fashion by changing the neurons deinactivation threshold E_h in relation to its resting potential E_L.

In our reticular neurons the resting potential lies below its deinactivation threshold. This means that the neuron will be effectively hyperpolarized at rest. For our reticular neurons to spike tonically constant depolarizing input is required to keep the neuron from going back to resting level and t-channels deinactivating. Furthermore, under resting conditions sporadic excitation leads to the emission of bursts with a high probability similar to observations in vivo [42].

In contrast, in the relay neurons the deinactivation threshold lies below the resting potential. At rest these cells do not deinactivate t-channels. Correspondingly, sporadic excitation does not lead to bursts but can only trigger tonic spiking. Active inhibition by means of GABAergic synapses, on the other hand, can effectively hyperpolarize these neurons and lead to the deinactivation of t-channels. Release from hyperpolarization then activates the channels and leads to bursts.

In conclusion, our neuron model exhibits the following characteristics. Thalamic reticular neurons can only burst in response to excitation, if the background afferent excitation is low enough to allow the passive leak currents to hyperpolarize the cell below the t-channel threshold. Thalamic relay neurons can only burst after release from a period of active inhibition. The relationship of the parameters and thresholds is illustrated in Figure 4.1.

Example traces from two representative model neurons are shown in Figure 4.1D.

4.3 Results

4.3.1 Normal

In order to get a realistic estimation of the free parameters in the model it is important to benchmark the network behavior against data collected in vivo and in vitro. The mammalian thalamic network in its simplest setup should be able to produce two different regimes, one relating to the desynchronized tonic mode that carries information faithfully from the periphery to the primary sensory areas in the neocortex and one mode relating to sleep oscillations. The latter has been hypothesized to be based on intrathalamic network interactions. We use these modes to calibrate the system. Manipulations carried out to reproduce the pathological network states are based on the same parameter sets as in the healthy tonic and sleep modes.

Tonic state

The thalamus is the central hub that transmits information from the periphery to the primary cortical areas. In the awake monkey, thalamic neurons in primary relay nuclei tend to spike tonically [102]. Stimulus dependent activation in afferent fibers should then lead to proportional activation in thalamic neurons with a minimum of bursting. The awake healthy state is defined as the parameter set that shows tonic spiking in response activation from the periphery in combination with a minimum amount of bursting. This behavior can be seen in Figure 4.2A. Neurons spike tonically in a decorrelated fashion. Oscillations are small because the recurrent negative feedback from RTN to the relay nuclei is comparatively small with tonically spiking RTN cells.

Spindle sleep

Sleep rhythms are a classic example of rhythmic oscillations found in the mammalian thalamus. A special case are the spindle sleep oscillations that occur at the transition from wakefulness to sleep. The underlying mechanisms have been investigated in many studies both theoretically and experimentally [7, 25, 37, 44, 128]. The oscillations observed in the EEG of sleeping subjects are assumed to be generated by the intrathalamic feedback loop between thalamic relay and reticular nuclei. This loop becomes active especially under conditions of neuronal hyperpolarization, which leads to increasing amounts of bursting as discussed above. Neuromodulation by deep brain nuclei has been

hypothesized to be responsible for a shift of the thalamic neurons resting potentials at the onset of sleep [36]. Bursts in the thalamic relay and reticular nuclei have been shown to efficiently recruit and drive each other [37]. Burst in the thalamic reticular neurons can cause strong prolonged inhibition in the reciprocally connected relay neurons. Upon release of this inhibition a rebound burst is triggered, that excites the reticular neurons and re-initiates the cycle. The circuits that are engaged in this oscillation are synchronized by divergent intrathalamic connections as well as cortical feedback. Spindle oscillations have been shown to occur at a frequency between 7 and 14 Hz.

The current model provides a correlate of spindle-like oscillations at a frequency of roughly 10 Hz under conditions of decreased cortical excitation in the RTN (Figure 4.2B). The reduced RTN activation leads to hyperpolarization in individual RTN neurons and hence more burst firing (Fig. 4.2D). The resulting bursts are very effective in driving rebound bursts in the SP and especially the NSP relays. Divergent connectivity is able to synchronize the bursting behavior and the resulting network oscillation shows highly synchronized peaks occurring every 100 ms (Fig. 4.2C). The interburst interval is dependent on the time-course of reticular inhibition on the thalamic relay in combination with the time-constant τ_{h2}. Note that RTN and NSP neurons are bursting on almost every cycle of the oscillation. The 10 Hz measured here can be considered to be the frequency with the maximum amount of bursts as determined by the physiological properties of thalamic neurons.

The spindle-mechanism shown here is akin to the network behavior observed by other researchers [37]. The factor that leads to a transition of the system's state to spindle-like oscillations is relative hyperpolarization in the reticular nucleus. In vivo, this is likely to be based both on a decrease of cortical input as well as changes in the neuromodulatory climate at the onset of sleep [36].

The classical waxing-and-waning structure of spindle oscillations is largely absent in the data shown in Figure 4.2. This is not surprising since the envelope observed in spindle oscillations is usually attributed to calcium-deactivated cation currents [32] that are not present in our neuron model. However, the current model has an interesting feature that can produce waxing-and-waning envelope oscillations without the inclusion of more ion channel types. Under certain parameter settings the oscillations produced by the model can interfere with the burst generating mechanism. The more synchronized the oscillation the less neurons are recruited in bursts. This leads to an overall delayed desynchronization which produces a waxing-and-waning structure to the 10Hz spindle oscillations (data not shown).

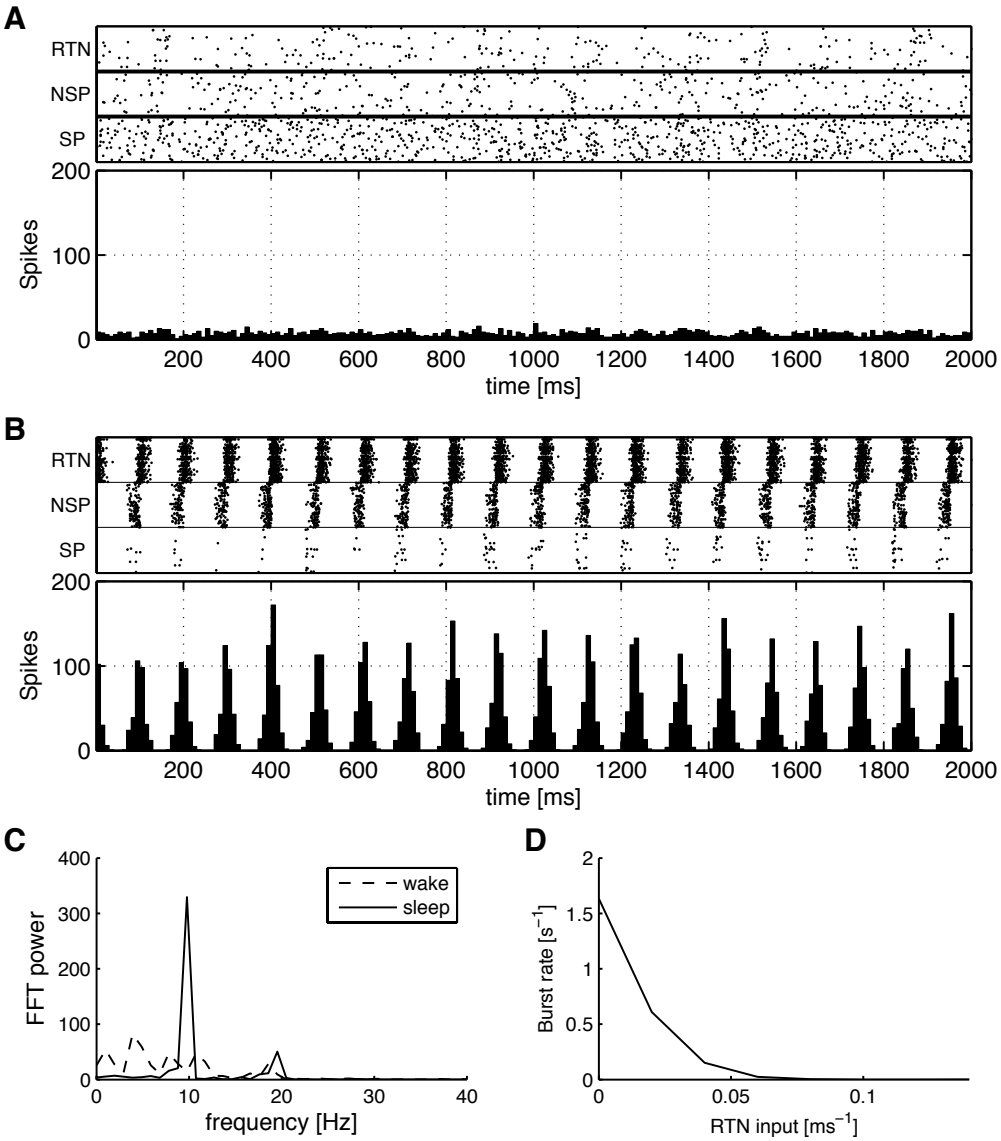

Figure 4.2: Model behavior under different activity regimes. (A) shows a spiking activity raster of the model under awake parameters with the PSTH activity in 10 ms time bins. Decreasing the excitatory random input leads to synchronized oscillations (B). These typically occur at a frequency of 10 Hz (C), independent of model parameters. (D) shows the relationship between the number of LTS bursts occurring in the model and the amount of random input into RTN.

The transition to oscillations in the delta frequency band, associated with deeper sleep states is not reproduced by the current model as it is dependent on complex interactions of network activity with metabotropic GABA receptors not simulated here.

4.3.2 Dysrhythmia

Neurogenic pain in thalamocortical dysrhythmia is triggered by a local decrease in excitatory afferent thalamic input. It has been suggested that this has a direct effect on the reticular nucleus in which neurons are particularly sensitive to decreased levels of excitation [63]. Because the resting potential of model RTN cells lies below the threshold for deinactivation of calcium channels, the decrease in activation in combination with sporadic cortical excitation is a potent burst generating mechanism. This is comparable to the change in excitation during the sleep state of the model. In contrast, in the TCD state the input to a number of thalamic relay cells, both specific and non-specific, is cut while others are left intact. Whereas in the sleep model the input from cortex to RTN was decreased, in the TCD state this occurs in an indirect way, by decreasing input to local areas of SP and NSP. These deafferented areas are ideal breeding grounds for low-frequency bursting oscillations, as they not only lead to hyperpolarized RTN neurons but are also especially prone to produce rebound bursts in response to recurrent RTN inhibition. If a critical mass of neurons are engaged in this oscillation the rebound inhibition from RTN can be strong enough to overcome the excitation present in unaffected areas of NSP by means of the divergent RTN→NSP connections and lead to a spread of the oscillation to other previously unaffected areas of the thalamic relay.

In Figure 4.3 we cut 20% of the afferents to both the specific and non-specific thalamic relays. This leads to a subsequent entrainment of the unaffected parts of the network. Furthermore, in the non-specific relay there is an overall increase in the bursting activity even in unaffected regions.

This bursting occurs at a frequency of 5 Hz in correspondence with electrophysiological measurements in patients suffering from TCD [83, 66]. The specific oscillation frequency is lower than during the spinde-sleep rhythms as generally less neurons are involved in the oscillation and the net inhibition from reticular neurons to the relay neurons is lower. The overall system is more noisy due to the aberrant excitation from unaffected neurons interfering with the oscillations. This reduces the oscillation frequency to pathological levels.

Crucial for the development of bursting and hence synchronized oscillations is the deafferented area in the NSP. Consequently, lesions in this area are

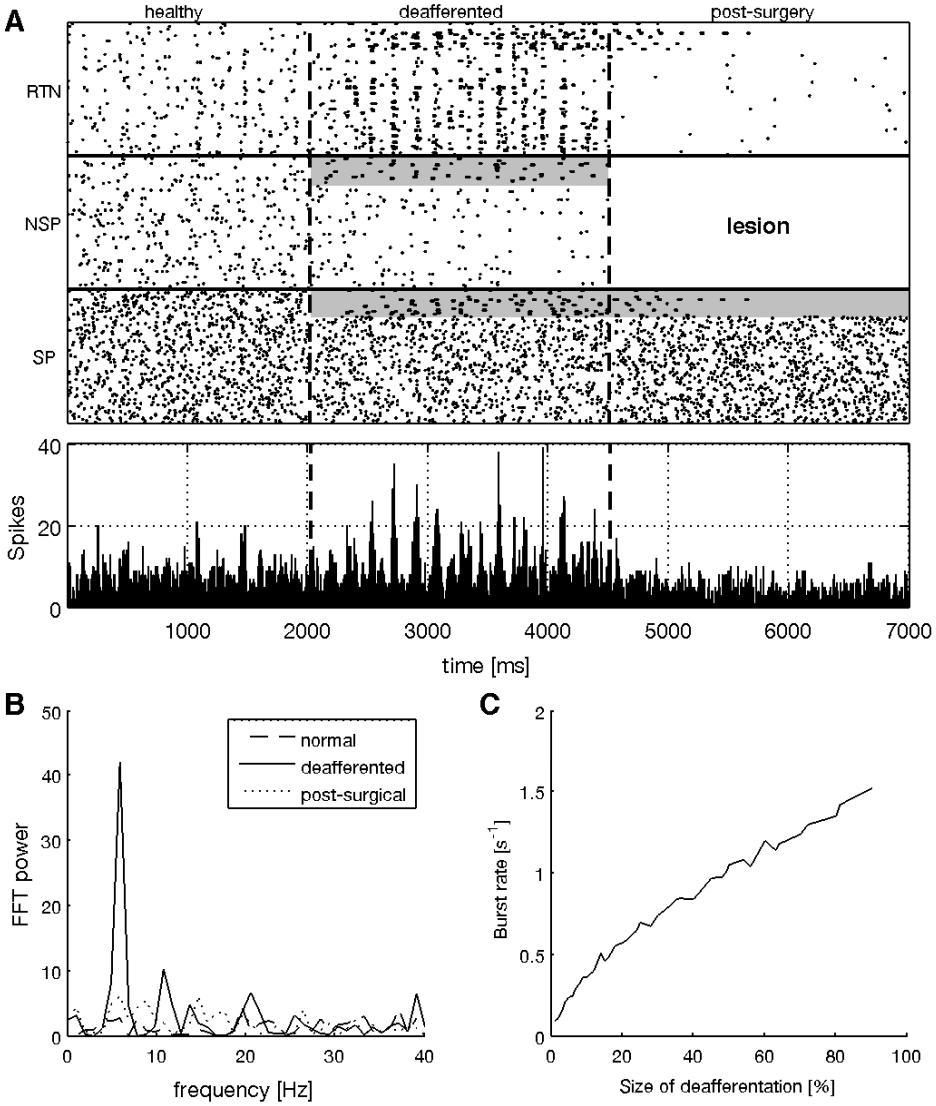

Figure 4.3: (A) Spiking activity raster under three different regimes (dashed vertical lines indicate parameter transitions). Selective deafferentation of relay neurons leads to TCD-like states with relay oscillations around 5Hz. (B) Fast Fourier transformation of spiking activity of the thalamic relay neurons. Switching off the non-specific nucleus rescues the system. (C) shows the amount of bursts in all three neuron groups with different amounts of deafferentation. At 100% deafferentation the network is silent.

the most effective in decreasing the amount of pathological bursting and low-frequency oscillations. This is shown in Figure 4.4. The efficiency of lesions in NSP is dependent on the amount of overlap this lesion has with the deafferented area. This is consistent with clinical observations.

4.3.3 Controls

Two factors shape the activation regime of the model. Firstly, the amount of afferent excitatory input puts thalamic neurons in one of three states: tonic spiking, bursting, or quiescence. These modes have been explored above. The intrathalamic connectivity is then responsible for the generation of synchronous rhythms or decorrelated activity, depending on the efficacy of intrathalamic synapses as well as the network topography.

The activity regimes shown here are based on the assumption that thalamic bursts are ideally suited to recruit bursts in other neurons via intrathalamic connections. Tonic spikes on the other hand are not. The network is therefore set up in the following way.

First, excitatory input to RTN is strong and abundant enough to prevent burst responses in RTN neurons. The required excitation stems from both peripheral sources via the SP/NSP thalamic relays or from cortical areas above.

Second, recurrent inhibition from RTN to SP/NSP is strong enough to recruit rebound bursts but only if the presynaptic neuron is bursting itself. Furthermore, the peripheral excitation needs to be balanced with the recurrent inhibitory feedback. In the current model, inhibition is generally stronger from RTN to NSP than RTN to SP. This is mediated by the larger number of connections between RTN and non-specific thalamic nuclei [122]. This means that in a heterogeneous state such as the dysrhythmic model activity, in which some neurons are deafferented and others are not, RTN bursting feedback is able to recruit thalamic relay bursts in NSP but not in the unaffected parts of SP. In the homogeneous sleep state, on the other hand, the amount of feedback is enough to overcome excitation even in SP leading to oscillations recruiting the whole thalamus.

In Figure 4.5 we show this interdependence of excitatory relay-reticular and inhibitory reticular-relay connections. Bursting occurs as an interaction of excitation and inhibition as the feedback loops are recruited in bursting oscillations.

4.3.4 Extrapolation

One feature of the model presented above is that it allows extrapolation to other types of treatment for the symptoms associated with thalamocortical dysrhyth-

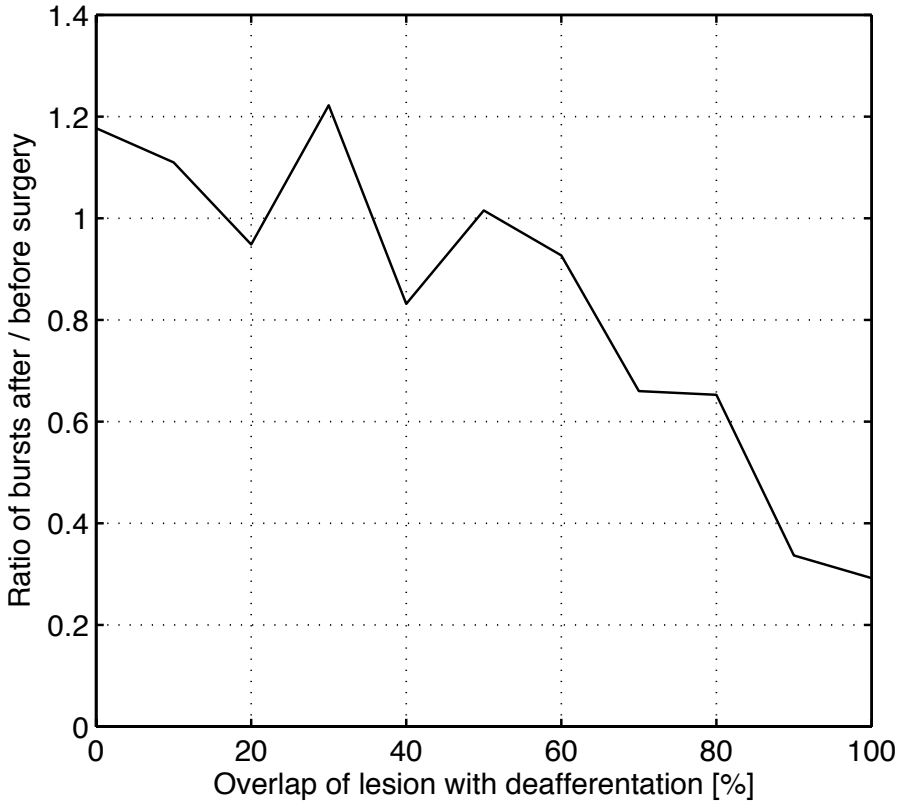

Figure 4.4: Effect of the location of the lesion. The more the surgical removal of NSP overlaps with the area affected by the deafferentation the better the improvement of the post-surgical condition in terms of the amount of bursting in all thalamic nuclei.

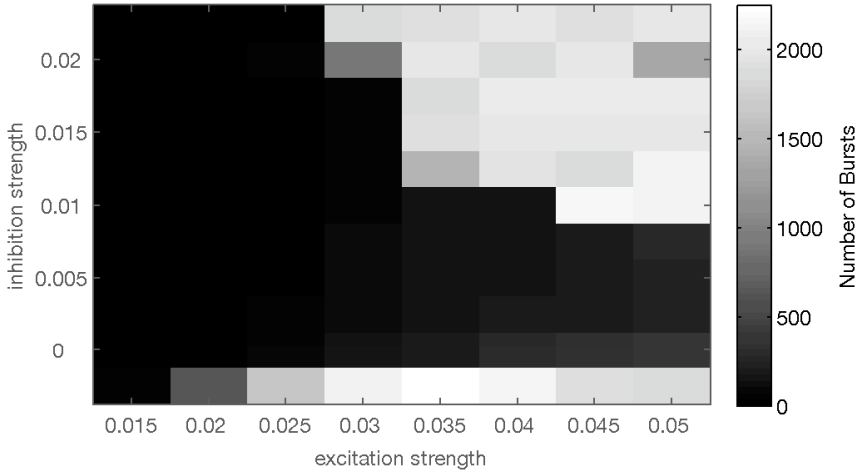

Figure 4.5: Effect of connection strength between thalamic nuclei. Lighter areas signify more bursts. The light area at the bottom corresponds to extreme activation of the model with very high spiking frequencies, undistinguishable from bursts.

mia. Phantom limb pain is a special case of neuropathic pain that is characterized by severe pain after the amputation of a limb. In some patients the pain sensation can be chronic and resistant to conventional therapies.

The famous mirror box by Ramachandran and colleagues provides patients suffering from phantom limb pain with visual input of a healthy hand [101]. This input is showing a mirror image of the healthy hand in place of the amputated hand to the patient. CL is known to receive multimodal input and it is hence feasible that visual input from the amputated hand will depolarize deafferented areas in CL. This depolarization can counteract the generation of low-frequency bursting oscillations by indirectly preventing hyperpolarization in RTN. This is shown in Figure 4.6. After the deafferentation phase, external excitatory spikes are fed into the NSP and replace the missing input from the deafferented limb. RTN neurons are depolarized and switch from the pathological bursting back to tonic spiking.

Note, that under these conditions bursting occurs in the deafferented SP-RTN circuits. Overall bursting in the thalamus is decreased by the excitatory input and there is less synchrony due to the NSP-RTN circuits not being involved.

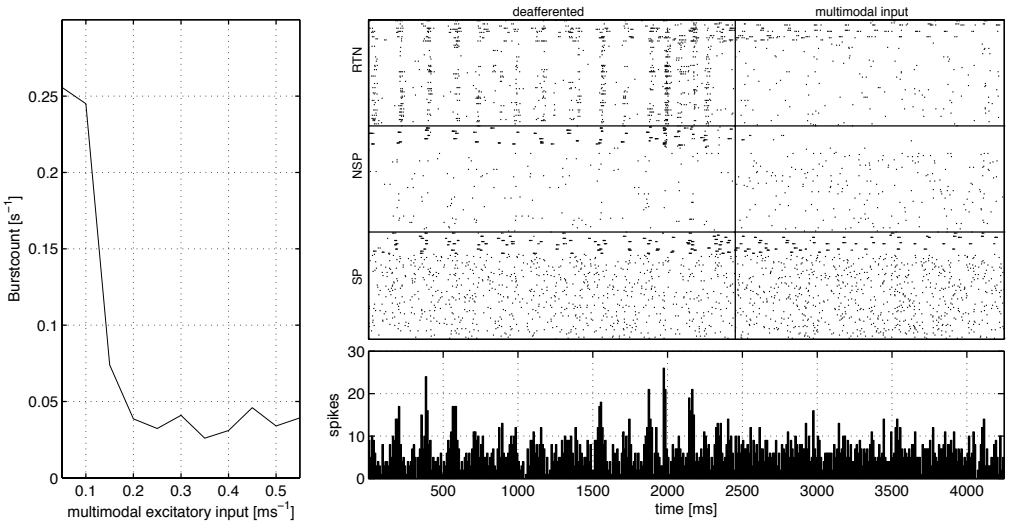

Figure 4.6: Multimodal excitation rescues the system. Left panel: The more excitatory input the stronger the decrease in the amount of bursts. Right panels: example spike plot and PSTH of a deafferented, dysrhythmic system, rescued by multimodal excitation delivered to NSP. The vertical line marks the onset of stimulation.

4.4 Discussion

We have shown a biologically inspired computer model of the mammalian thalamus that is able to switch between different activation regimes in response to physiological and pathological manipulations. Furthermore, we are able to capture a number of prominent phenomena with a highly simplified neuron model and network architecture. The proposed mechanisms might explain the robustness of both healthy and pathological oscillations in the thalamocortical system.

The data presented here has a number of interesting emergent features that are also found in in vivo studies of the same system.

Firstly, the network oscillations produced by manipulations in both the healthy and pathological part of the model show the same frequency shifts as is observed in TCD patients. The sleep state is characterized by oscillations in the alpha frequency band. This is a direct effect of the physiological properties of the neuron model, namely the time-constant of t-channel deinactivation. Because the whole network is engaged in the oscillations the recruitment of individual cells can occur on each cycle with a high reliability. Hence the frequency approaches the maximum permitted by the physiological properties of the model neurons.

In the TCD state the oscillation frequency decreases towards the theta band. Here the number of neurons engaged in the generating mechanism of the oscillation is smaller than during the sleep state. Individual neurons are recruited less reliably with an overall decrease in synchrony. The recruitment of circuits is less tight and hence slower leading to an oscillation frequency in the theta band as is typically observed in patients suffering from TCD. In this scheme the theta rhythmicity is a direct effect of the noisy conditions in the awake brain.

A second feature of the model is that total deafferentation of the thalamus from peripheral inputs does not lead to TCD (Figure 4.3C). This is in accordance with the observation that TCD tends to be rare in quadriplegic patients in which a large part of the somatosensory inputs have been deafferented. In the model, this is based on the fact that RTN neurons need sporadic excitation from the thalamic relay areas SP/NSP to start the recurrent bursting mechanism.

Thirdly, in the current model, the deafferented NSP area is the driver of the oscillations that can then recruit larger thalamic areas. It is here that the most bursts occur and it is also this region that needs to be silenced in order to achieve recovery from the TCD state. This is consistent with data from studies looking at the amount of bursting in patients suffering from neuropathic pain. Here, the most bursting has been found in the posterior part of CL and this has also proved to be the most efficient target for surgery [71, 62]. In comparison, in the model the factor that determines the efficacy of the surgery is the amount of overlap of the lesion with the deafferented areas (Fig. 4.4).

Fourthly, the model captures the observation that there is generally more bursting in the non-specific parts of the thalamus than in specific neurons [71, 83, 102, 63]. In general, the RTN inhibition triggered by the increase in bursting has a larger inhibitory effect on the NSP parts and hence is able to overcome the incoming peripheral activation even in parts that are not affected by the deafferentation. In comparison, the SP part of the model is only affected in the deafferented region. The remaining peripheral activation is not overcome by the burst triggered RTN$\rightarrow$SP inhibition, hence allowing spared signal transduction from periphery to primary sensory cortex. This is in accordance with in vivo observations from patients in which specific somatosensation is spared in the body parts that have not been deafferented. The increase in bursting in the non-specific thalamic areas, on the other hand, provides a fitting correlate for the affective dimension of pain thanks to thalamocortical and corticothalamic divergence of the paralimbic system.

Fifth, the current model is sensitive to the amount of cortical excitation reaching the reticular nucleus after surgery. At low levels of cortical excitation the model is not able to recover from the bursting mode and hence the rhythmic

oscillations carry on indefinitely. In the clinic, the functional neurosurgical intervention is in the majority accompanied with psychotherapeutic treatment of the patients. It is feasible that this treatment adds to the amount of associative non-specific activation that reaches the RTN and NSP from paralimbic cortical areas.

Apart form replicating patterns of observations from patients the model also enables us to generate testable predictions about TCD and its therapies. Mainly, the models' behavior is dependent on the net afferent excitation in the different areas of our thalamic model nuclei. The relative amounts of incoming excitatory spikes allow for the generation of bursts on the one hand and the cessation of oscillations after surgery on the other hand. In general, we make the prediction that desynchronized excitation is beneficial to the prevention and recovery of TCD as it limits the amount of bursts that are being generated in the thalamus. Furthermore, the current model is sensitive to both the specific connectivity pattern between NSP and RTN. Our simulations have kept this pattern constant, but changes in the connectivity can have large effects on the model behavior. It is feasible that there are certain connectivities that are more beneficial to the generation of TCD than others. This could explain the fact that not all deafferentations lead to symptoms of the TCD type. Perhaps a genetic predisposition could be manifested in the density of connections between thalamic reticular and non-specific thalamic nuclei. Along the same lines the efficacy of GABAergic synapses in the thalamus play an important role in the generation of rhythmic oscillations. A minimal strength of inhibition is crucial for the development of self-reproducing bursting oscillations. This could be tested by specifically altering GABAergic inhibition in the thalamus by pharmaceutical means. In fact, many epileptic drugs work as GABA antagonists.

In the interest of simplicity, here, I have abstained from closing the thalamocortical feedback loop that has been shown to be involved in the spread and synchronization of brain states such as non-paradoxical sleep. The burst generation mechanism employed by our model is easily extensible with cortical feedback in that the reentrant excitation is likely to be highly correlated with efferent thalamic excitation. Since the RTN neurons are particularly sensitive to rhythmic excitation, closing the thalamocortical loop is likely to produce stable rhythmic states.

This is also bound to have consequences on the balance of excitation and inhibition in the cortex and might be used to model the generation of positive symptoms of TCD through corticocortical inhibition [78].

Chapter 5

Cortical Activation and Positive Symptoms in TCD

5.1 Introduction

In the previous chapters we have seen how small changes in the input statistics to the specific and non-specific nuclei of the thalamus can lead to drastic changes in the behavior of thalamic neuron populations. Decorrelated tonic spiking activity can be transformed into highly synchronous slow frequency oscillations. The state of the thalamic system will have a strong effect on the activity of neurons in the overlying layers of cortex.

Thalamic nuclei project mainly to layers IV and VI of the cortical sheet. The neurons in layer VI are assumed to be projecting straight back to the thalamus, thereby closing a direct feedback loop. This has been argued to be an important factor in the synchronization and spread of sleep rhythms [25]. Neurons in layer IV on the other hand are a hub for intracortical connectivity. The neocortex is widely accepted as the seat of higher cognitive function in the brain.

In the same way that the thalamus is responsible for the generation of low-frequency rhythmicity in TCD, interactions at the level of the cortex are responsible for the development of symptoms like pain, tremor, tinnitus etc. These symptoms are known to clinicians as positive symptoms because they indicate increased levels of activity in affected areas of the brain. Here we run into a paradox. How is it that the slowing of oscillations coupled with long periods of decreased activity associated with thalamic throughput in TCD can lead to an overactivity in the cortex?

The answer to this question lies in the dense interconnectivity between neurons in the cortex. Primary sensory cortices of different modalities have been

shown to include both excitatory and inhibitory connections. These can then lead to the shaping of spatiotemporal receptive fields and the propagation from one stage of sensory processing to the next.

Excitatory and inhibitory neurons balance afferent activation in the cortex to provide stable activity without complete suppression or activation. The switch from healthy activation to TCD activation has been assumed to alter the balance between excitation and inhibition in a way that produces aberrant activation in areas adjacent to the ones affected by the TCD [77, 78], called edge effect [49]. This hypothesis is based on the change of inhibition between affected and healthy thalamocortical columns. Low-frequency activation is supposed to be less efficient in driving inhibitory networks than high-frequency activation. Low-frequency in one column will hence lead to a decrease in inhibition in the neighboring columns. Furthermore, this decrease of inhibition will cause an increase in activation which in turn serves to inhibit the low-frequency column even further. This has been termed the edge effect in TCD [78].

Unfortunately, authors of previous papers describing this phenomenon have not been clear about what features of the altered thalamocortical stimulation is causing the edge effect, mixing up net activity with dynamical factors [78]. Net activity, is the overall effect that activity spikes at low-frequencies will carry less energy than activity spikes at high energies. Even if one takes into account the efficacy effects found at thalamocortical synapses in layer VI in response to thalamic bursting [15] there will overall be less excitatory synaptic events than under awake gamma oscillations. The dynamical effects of changing oscillation frequency are less clear. Different spike times can have significant impact on intracortical synchronization and hence spiketime-dependent plasticity effects.

In vivo, there are a number of complicating factors. Firstly, of course excitation and inhibition coexist in cortex. A decrease in activation in TCD-affected columns will therefore also have an effect of decreasing lateral excitation - counteracting the effect of decreased inhibition. In order for an edge effect to occur it is therefore necessary to introduce heterogeneous excitation and inhibition. Indeed, it has been shown that - at least in primary visual cortex - inhibitory connections tend to terminate in close proximity to the presynaptic neuron, whereas excitation tends to be sparser and connect in a more widespread fashion.

A second complicating factor is the dynamical component referred to above. It is not only the net activation that matters but also the temporal structure of the input. Cortical neuron ensembles in the awake brain tend to oscillate in the gamma frequency range. This is likely based on the specific membrane time-constants and synaptic dynamics in cortical excitatory-inhibitory networks. This will not only change the effectiveness of input during different phases of the

oscillation but can lead to harmonic effects as well.

Here we want to investigate on the one hand what neural architectures can support an edge effect as has been hypothesized in the literature. Furthermore, we want to take a closer look at the dynamical effects that might be involved in such a mechanism.

5.2 Abstract model

Cortical architecture tends to be more complex than the relatively homogeneous connectivity patterns found in the thalamus. For this reason accurate modeling of cortical processes requires a different approach than was used in the previous chapters. In order to gain a basic understanding of the interaction between manipulations of cortical stimulation and network architecture we need to choose a level of modeling that approximates our understanding of cortical function. In this section we will therefore model cortical activity in a more abstract form. We assume that cortical architecture is clustered into small functional units with dense internal connections along the lines of cortical microcolumns [40]. These units are functionally connected to surrounding areas by means of excitatory and inhibitory connections.

5.2.1 Model setup

Unit definition

Instead of modeling the spiking dynamics individually we will firstly resort to a mean field approach, assuming that activity levels within functional units will not differ significantly amongst each other. Units integrate incoming activity. In the absence of afferent input the activity of units dissipates exponentially:

$$\frac{dA_j}{dt} = -A_j/\tau + S_j + I_{ext} \tag{5.1}$$

with A being the units activity level and τ being the membrane time constant of the unit. S represents the synaptic input from the other units in the model and I_{ext} is the external input from thalamic and other sources.

$$S_j = \sum_{i=1}^{N} f(A_i w_{ij}) \tag{5.2}$$

where $f(x)$ is an arbitrary function of the input-output relationship of the model units, which is here assumed to be

$$f(x) = \begin{cases} x & \text{if } x > 0, \\ 0 & \text{if } x \leq 0. \end{cases} \tag{5.3}$$

and w_{ij} is the connection weight matrix from neuron i to neuron j.

Model connectivity

The connectivity employed here aims to capture the interplay between excitation and inhibition in the cortex. The general consensus about cortical connectivity at an abstract level is that local dense inhibition balances with sparse long range excitation. This is captured in a connectivity function described by a difference of gaussians (see Figure 5.1):

$$w_{ij} = \gamma_{exc} \frac{1}{\sigma_{exc}\sqrt{2\pi}} exp\left(-\frac{(i-j-\mu)^2}{2\sigma_{exc}^2}\right) - \gamma_{inh} \frac{1}{\sigma_{inh}\sqrt{2\pi}} exp\left(-\frac{(i-j-\mu)^2}{2\sigma_{inh}^2}\right) \tag{5.4}$$

where γ_x is the excitatory and inhibitory efficacy, and σ_x is the width of the gaussians. The quantity $i - j$ denotes the distance of individual nodes in the 1D model. This connectivity profile allows us to approximate different connectivity forms in cortex with a minimum of free parameters.

In the simulations presented next we connect together 100 units of the described type in a one-dimensional array. All simulations could of course be extended to involve two dimensions. In order to avoid boundary effects we wrap connectivity around at the borders.

Stimulation

The working hypothesis as initially proposed by Llinas [78] is that normally functioning units tend to oscillate at a frequency of roughly 40Hz. This is an interaction of intrinsic sub-threshold oscillations as well as thalamocortical resonance. We mirror this behavior in our model by supplying excitation to each unit with a frequency of 40 Hz. Each unit receives this activation unsynchronized with the other units, i.e. the phase of each stimulation is randomized at the onset of each simulation.

In the dysrhythmic brain, local areas of thalamus are deafferented and hence switch into a mode characterized by low-frequency bursting oscillations (see previous Chapters). The normal 40 Hz resonance is hence converted into a strong 4 Hz synchronized activation. We model this by changing the input activity of some *affected* units to occur at said 4 Hz.

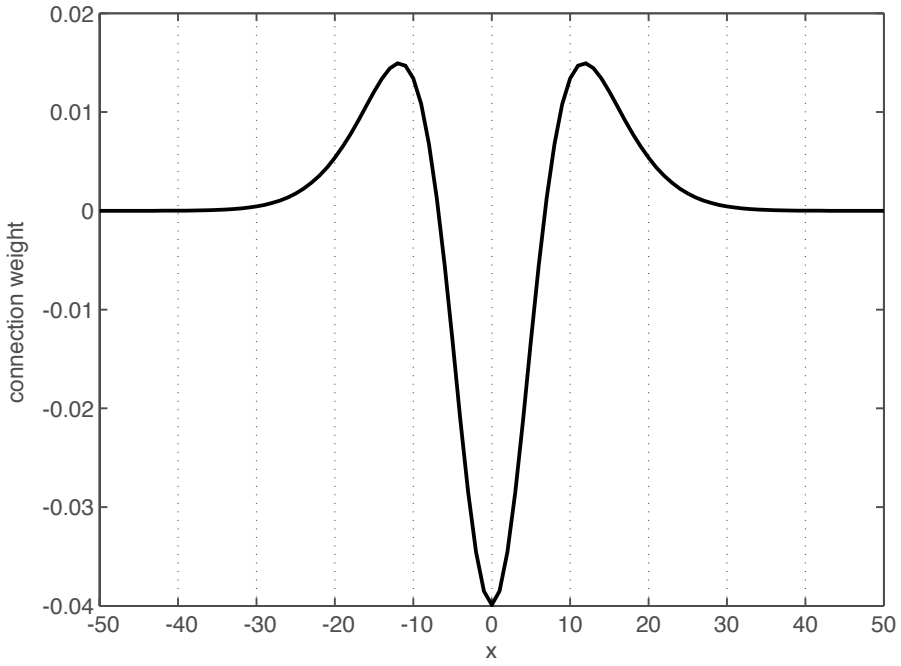

Figure 5.1: Typical example of a connectivity profile in the current model is estimated by a difference of Gaussians function that can be shaped by four independent free parameters ($\sigma_{exc} = 10; \sigma_{inh} = 5; \gamma_{exc} = 1; \gamma_{inh} = 1$).

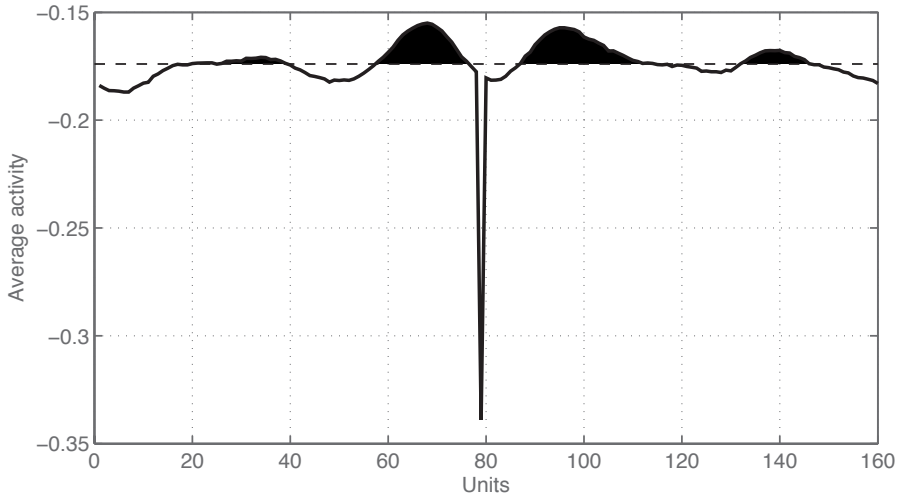

Figure 5.2: Profile of average activity of each unit after 3s model time. The unit affected by the dysrythmic low-frequency input (unit 79) affects the surrounding units to show a halo of overactivity that is the edge effect. We quantify this by measuring the area between the profile and the average activity (dashed line) marked in blue, but neglect the decrease of activity caused by the edge effect in other regions. (N=200)

5.2.2 Measuring the edge

In the following investigations we will need to quantify the edge effect in relation to the free parameters of the model. For this we measure the increase of activity levels from baseline outside of the central depression area caused by the dysrhythmia. This is illustrated in Figure 5.2. Lower levels of excitation in one neuron will systematically change the input to its postsynaptic units, depending on its connectivity profile. The short-range inhibition will be decreased leading to an increase in activity in the areas in its immediate vicinity. Furthermore, a decrease in excitation coupled with an increase in inhibition of more distal connected units causes lower activity in distal areas.

5.2.3 Results

Edge effect demonstration

We firstly want to demonstrate the edge effect in a model setup as described above. We implement a connectivity profile of short inhibition and long excita-

tion and excite all units with activity spikes at a frequency of 40 Hz. Units are here assumed to be desynchronized and have a random phase difference. One unit in the center of the network receives a 4 Hz input instead of the 40 Hz input. This changes the balance between lateral excitation and inhibition in the immediate vicinity of this dysrhythmic unit, leading to a halo of over-activity. This is the edge effect in a static setting. Note that synchronization and frequency effects do not affect the model behavior apart from a change in net activity. In the following paragraphs we will investigate the behavior of this model in response to the manipulations of a number of free parameters. It is also important to note at this point that the effect is a consequence of altered balance between model units. The underlying assumption is that in a normal state the activity of cortical units balances with the activity of other units, only allowing peaks and troughs in response to external stimulation. In the resting state the model should be in equilibrium. The change in input dynamics under pathological conditions can then lead to a systematic bias in activity of some units. This is manifested here in the form of the edge effect.

Noise

In addition to the regular 40/4 Hz stimulation of the model it is also possible to simulate more realistic conditions by introducing noise. The effect that this noise will have on the edge effect is not easy to predict. On the one hand, noise can have a depolarising effect on deafferented areas thereby decreasing the amount of disinhibition on the edge. On the other hand, the extra input stimulating unaffected units will also lead to more inhibition in the deafferented area with a potential to exacerbate the edge effect by leading to even lower activation levels. We investigated this systematically with the model by changing the amount of white noise stimulation of all units in the model. Results are shown in Figure 5.3. The amount of noise increases the amount of excess edge-activation linearly.

Size of affected area

The size of the area affected by the TCD, i.e. the size of the area receiving 4Hz instead of 40Hz input, has a marked effect on the strength of the edge effect. The more units are subjected to the low-frequency input excitation the stronger the disinhibition on neighboring areas. Furthermore, inside the epicenter there can now be disinhibition effects triggered by excitation from distal units that are met with a strong decrease of inhibition within the affected area. This is

illustrated in Figure 5.3. The strength of the edge increases with the size of the deafferented area.

Range of excitation vs inhibition

In the simulations shown above we have resorted to the classical proximal inhibition against distal excitation connection profile. This setup is beneficial to the existence of an edge effect as it emphasizes inhibition over excitation in the difference of gaussian connectivity (wide Gaussians will have a lower peak than narrow Gaussians). In order to investigate the effect that specific connectivity has on the edge effect we can alter the relative strength of inhibition versus excitation in the model. The results are shown in Figure 5.4.

The saturation seen in the Figure is based on the strength of relative excitation. A gaussian of lower width has a higher amplitude. This introduces a large amount of excitation into the model, more than can be balanced with the longer range inhibition. This could in theory be counteracted by increasing the amplitude of inhibition in relation to the excitation.

5.3 Edge effect in a spiking network model

The simple model described above exhibits stable edge effects for all connectivity patterns as long as excitation is less local than inhibition (Figure 5.4). An abstract model like the one described above requires a large amount of simplifying assumptions regarding the inter-unit connectivity and the homogeneity of intra-unit neurons. In order to investigate the effect of single-neuron dynamics on the edge effect we extended the abstract model to incorporate spiking excitatory and inhibitory neurons.

Neuron model

In order to investigate dynamical effects in the interplay of different types of cortical neurons we need to employ a cell model that captures the different dynamics of these neurons while at the same time limiting the number of free parameters.

The neuron description by Izhikevich [58] fulfills these requirements. Each neuron is based on a simple two-dimensional system of differential equations described by

$$\frac{dv}{dt} = 0.04v^2 + 5v + 140 - u + I_{syn} \tag{5.5}$$

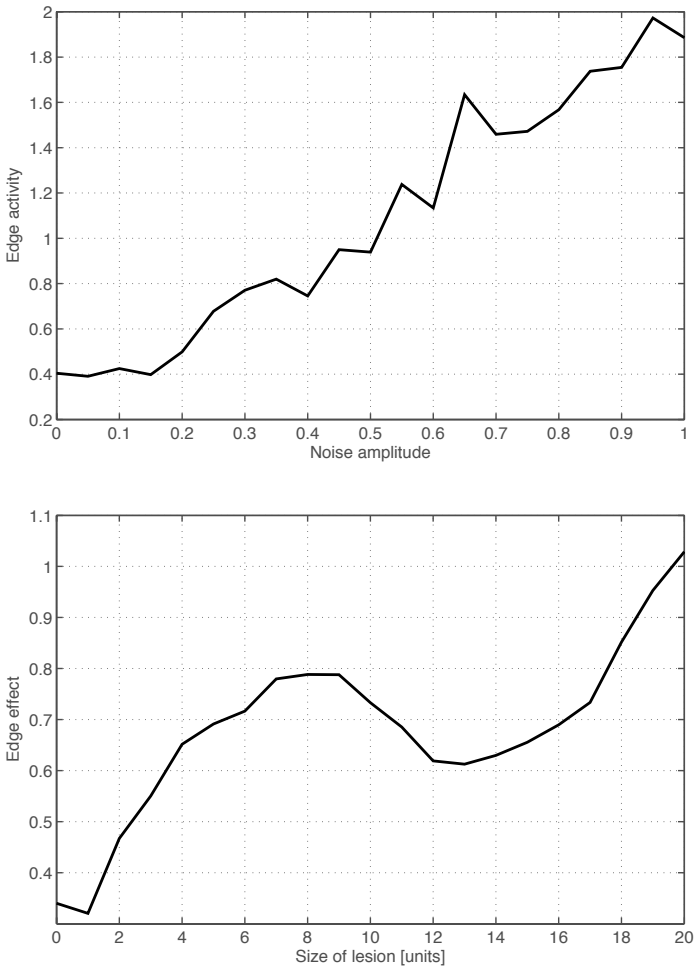

Figure 5.3: The effect of the size of the TCD-affected area and noise on the edge effect. Top: Increasing the strength of the noisy excitation exacerbates the edge effect. Bottom: Increasing the size of the deafferented area also increases the edge effect, albeit non-linearly.

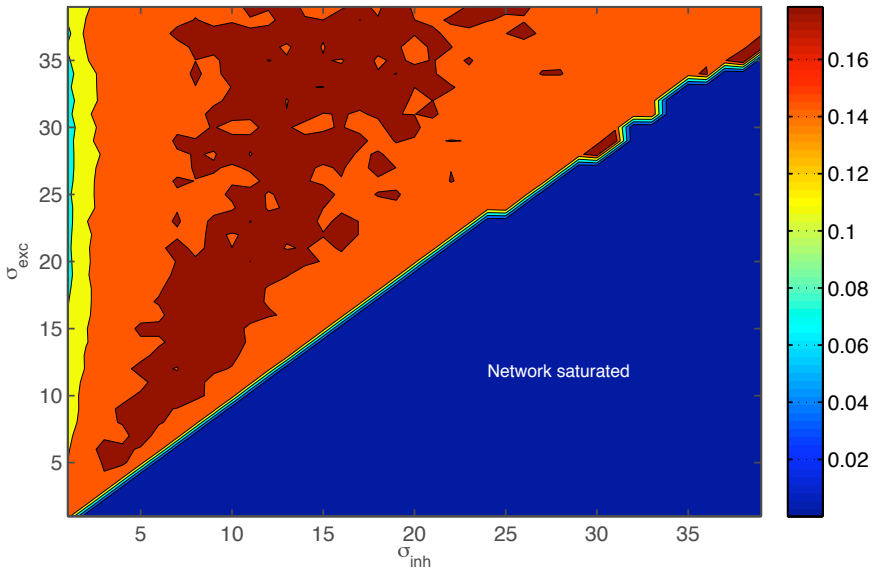

Figure 5.4: The range of excitation and inhibition has a direct effect on the strength of the edge effect. If inhibition is longer range than excitation the network saturates. In contrast, the edge effect is produced ideally by a value in the middle of the non-saturated zone.

Dynamics	A	B	C	D
Regular-spiking	0.02	0.2	-65	8
Fast-spiking	0.1	0.2	-65	2

Table 5.1: FS/RS parameters of Izhikevich neurons.

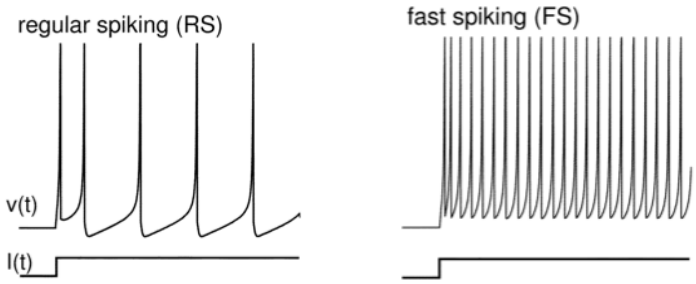

Figure 5.5: FS/RS dynamics of Izhikevich neurons [58]. Regular-spiking neurons show adaptation and overall lower firing frequencies under equal stimulation than fast-spiking neurons.

$$\frac{du}{dt} = a(bv - u) \tag{5.6}$$

Similar to the integrate-and-fire neurons described above the neurons membrane potential v and the recovery variable u are reset after every spike so that

$$\text{if } v \geq 30 \text{ mV, then } v = c \text{ and } u = u + d \tag{5.7}$$

In this way the behavior of the neuron model can be completely characterized with four parameters a, b, c, and d (see [58]). We chose parameters (Table 5.1) to model both regular spiking (RS) and fast spiking (FS) behavior (Figure 5.5). Regular spiking neurons exhibit tonic spiking with adaptation whereas fast-spiking neurons have lower thresholds and don't adapt their spiking rate to prolonged stimulus exposure. We assume that excitatory cortical neurons are of RS-type and inhibitory interneurons are of FS-type.

Network architecture

Our network consists of 2 layers, one containing 16x16 excitatory and the other containing 8x8 inhibitory neurons. This preserves the ratio of 4:1 cortical ex-

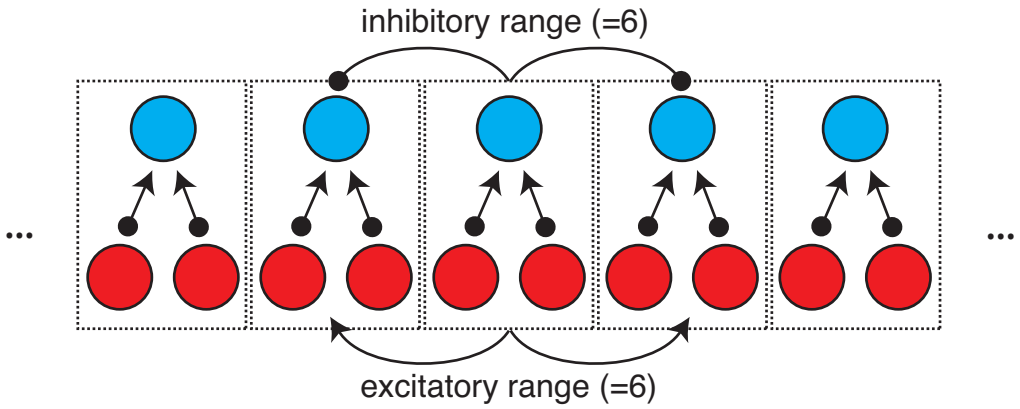

Figure 5.6: Network architecture in spiking model of neocortex (1D representation for simplicity). Red circles represent excitatory and blue circles inhibitory neurons. Each cortical module (enclosed by dashed line) consists of 4 excitatory and 1 inhibitory neuron that are reciprocally connected. Interactions happen by means of lateral inhibitory and excitatory connections with excitatory and inhibitory range expressed in terms of excitatory neurons. Round arrows: inhibition, sharp arrows: excitation.

citatory to inhibitory neurons as observed throughout mammalian cortex. We represent a cortical column by a quadruple of excitatory neurons reciprocally connected to one inhibitory neuron (see Figure 5.6).

Cortical columns interact by means of excitatory and inhibitory lateral connections, the range of which will be manipulated in the following experiments.

5.3.1 Edge measure

Similarly to the above section we define the edge effect as overactivity in areas adjacent to a central TCD-affected area. All excitatory neurons receive random Poissonian excitation with a rate of $40s^{-1}$. The TCD-affected central 5x5 neurons then accordingly only receives synchronized input spikes at $5s^{-1}$ as is predicted from TCD burst generation. We now define the edge as a halo of 2-neuron width around the central affected 5x5 area. The pooled activity over a time of 10s is then compared to the average activity of the unaffected surrounding area (see Figure 5.7). An edge index is computed by dividing the ratio of average activity in the edge area with the activity in the surround. Hence an edge-index of larger than 1 indicates an edge overactivity. In order to statistically compare the activity levels in edge and surround t-tests were conducted

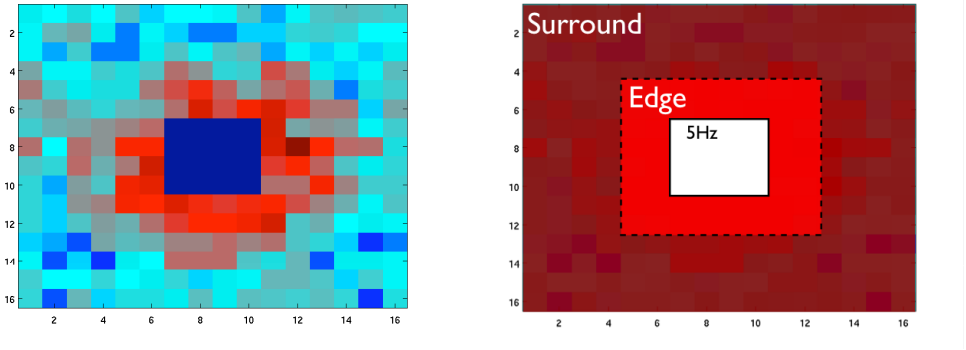

Figure 5.7: Edge effect in a spiking model of neocortex. Left: example depiction of summed activity in the excitatory model neurons. The hotter the color the more active the neuron over a 10s period. Right: Three areas are defined, TCD-affected (white), edge (red), and surround (dark red). The activity in the 16x16 layer of excitatory neurons is measured over 10s and then the ration between edge and surround is computed, resulting in an edge index.

between the activity of the edge and surround groups of neurons.

5.3.2 Results

Edge demonstration

When pooling the activity of excitatory neurons over a time course of 10 seconds an edge effect was clearly visible if we chose inhibitory connections to be wider reaching than excitatory connections (Figure 5.7 left). Note, that the current network architecture and connection width cannot directly be compared to the ones in Section 5.2.

The effect of excitatory range on edge activity

In order to investigate the effect of network connectivity on the strength of the edge effect we systematically altered the range of lateral excitation and inhibition between model columns while at the same time keeping neuron dynamics constant. In this experiment excitatory as well as inhibitory neurons were modeled by regular-spiking dynamics. Results are shown in Figure 5.8 (black bars). The significance and strength of the edge effect is clearly dependent on the lateral excitatory range. While keeping the inhibitory range constant at a value of 6, significant edge overactivation is seen for shorter ranges of excitation.

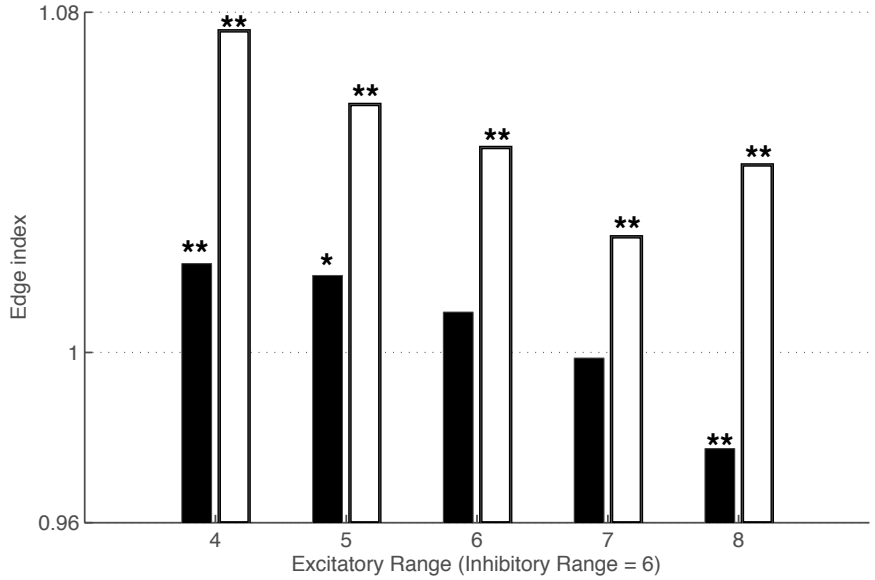

Figure 5.8: Edge effect and the interaction between network connectivity and neuronal dynamics. Changing the inhibitory neuron cell type from regular (black bars) to fast-spiking dynamics (white bars) increases the edge effect and makes it independent of network connectivity parameters. (Significance levels **: $p < 0.001$, *: $p < 0.05$)

If excitation is longer range than inhibition a negative edge effect can be seen (average index smaller than 1), with edge neurons being less active than unaffected surround areas.

The effect of neuron dynamics on the edge effect

Inhibitory neurons in the cortex tend to have different dynamics than excitatory neurons. While it is hard to make general comments about each cell type, as a working hypothesis researchers have modeled excitatory neurons as regular spiking with threshold adaptation while inhibitory interneurons were modeled by fast spiking neurons (e.g., [59, 58, 60]).

Inhibitory neurons of the fast-spiking type will have lower thresholds and will be able to follow fast stimulation regimes more readily than regular-spiking cells. Here, we wanted to investigate what effect this difference in neuron dynamics might have on the edge effect.

As can be seen in Figure 5.8 (white bars), introducing fast-spiking cell dy-

namics for inhibitory neurons exacerbates the edge effect significantly.

Furthermore, there is an interaction between cell dynamics and connectivity range parameters. Even under conditions which previously lead to negative edges (long excitation) the fast-spiking inhibition produces significant positive edges.

5.4 Discussion

Here we have shown the feasibility of edges in cortical architectures in response to changes in the statistics of afferent stimulation. Low-frequency stimulation can affect the balance between intracortical excitation and inhibition in a systematic fashion. We have used both an abstract mean-field model as well as a spiking neuron model to show some of the parameters that have a direct influence on the existence of cortical aberrant edge-excitation.

Our abstract model enables us to make predictions as to the relationship of the free parameters in the model: Firstly, the widely-assumed inverse mexican hat function of intracortical connectivity is ideally suited to produce edge effects. This is exacerbated by increasing overall activation levels. More activity leads to more lateral inhibition of unaffected areas further inhibiting the affected low-frequency stimulated areas. The current model predicts that an external stimulation of the TCD affected cortex will lead to a strengthening of symptoms in patients. It is important to note, however, that this might balance with activation effects in the thalamus shown in Chapter 4. The size of the affected area has a non-linear effect on the edge effect. While generally the prediction holds true that the larger the affected area the larger the edge effect there can be secondary areas of disinhibition within the low-frequency stimulated areas, if they are large enough. Lastly, we tested the effect of network connectivity on the edge effect. The simplified structure of the abstract model enabled us to quantify network connectivity with only two parameters. Edge characteristics were apparent when excitation had a longer range than inhibition. Under converse conditions the network saturated. This behavior is likely due to the dual effect that changing the width of individual Gaussian components has on the strength of the respective connections. The wider the connection width the lower the net excitatory/inhibitory effect. Hence, short-range inhibition and long-range excitation also inadvertently implement stronger inhibition than excitation - a condition that is crucial for the stability of the model. Since this setup is also likely to be implemented in the biological tissue we conclude that cortical architectures of this pattern are ideally suited to induce edge dynamics under TCD conditions.

In order to further investigate the properties of edge over-activation we extended the initial abstract results with a more biologically viable spiking neuron network model. Here we were able to reproduce lateral disinhibition without assumptions regarding cell dynamics only when lateral excitation exceeded lateral inhibition. The spiking model requires a delicate balance between excitation and inhibition in order to remain stable. Decreasing central activation caused by low-frequency TCD-like stimulation lead to a decrease in lateral excitation and inhibition since in the spiking model the two connectivity footprints overlap. The development of an edge in this connectivity profile relies on a imbalance between lateral excitation and inhibition. This is shown in Figure 5.8 where the lateral excitatory range in comparison to the inhibitory range is inversely and linearly related to the sign and size of the edge effect. In this scheme the model predicts that an edge effect is only possible if excitatory connections have a shorter range than inhibitory connections - a prediction that is at odds with current hypotheses about cortical connectivities.

One factor that attenuates this necessity is the spiking dynamics of the inhibitory interneurons in the model. When we switched these neurons to fast-spiking dynamics this lead to edge effects under all connectivity profiles tested. This is likely due to the fact that the FS dynamics disbalance the network and predispose lateral connections to have a net inhibitory effect on post-synaptic neurons. This counterweighs the effect of long-range excitation. The model predicts that FS spiking dynamics of interneurons is a contributing factor to symptom generation in patients suffering from TCD.

Overall, the wide range of parameters and network architectures that support edge behavior lead us to the conclusion that lateral disinhibition effects are indeed a ubiquitous phenomenon in the cortex. The persistence with which input statistics are altered in the case of thalamocortical dysrhythmia probably interacts with cortical plasticity effects to permanently engrave edge dynamics into the underlying structure.

Chapter 6

General Discussion

6.1 Summary

In the previous chapters I have presented a biologically inspired model of thalamocortical dysrhythmia, numerically simulating its genesis, its spread and decline as well as the generation of positive symptoms. While in some areas I have stuck to the initial descriptions of a TCD framework from the literature [77, 63], in some places I have altered and extended existing theory. It is notable how generic the mechanisms causing the TCD seem to be - even though our model architectures have been abstract and extremely simplified, replicating the physiological footprint of the TCD has been easy and did not require extensive parameter searches. While some of the data that went into the model design has necessarily been somewhat circumstantial, due to the tight ethical and temporal restrictions on data collection during surgery on humans, it has nevertheless been possible to build mathematical models of the ideas proposed by other researchers without conflicting with common physiological and anatomical knowledge.

Low-frequency bursting generation

In Chapter 3 I have looked at the genesis of low-frequency rhythms in a single thalamocortical column in response to manipulations to the afferent excitation. The notion that lack of afferent excitation leads to deinactivation of t-type Ca2+ channels has been implicit in all previous papers about TCD and yet has previously not been validated by experimental or theoretical work. In my model I have shown, how different inter-neuronal circuit setups can interact with the cell-intrinsic machinery to produce LTS bursts. Furthermore, I have identi-

fied and compared different hypothetical feedback circuits that could potentially serve to make such low-frequency oscillations rhythmic and persistent.

From my data, a cortical feedback loop that reinitiates thalamic bursting is unlikely due to the long delays necessary with such low-frequency activity. While a 25ms lag of recurrent excitation/inhibition is feasible to warrant the hypothesis that thalamocortical interactions are responsible for gamma rhythmicity in the brain, the long intervals of approximately 200ms between the LTS bursts would make a delay on a similar time-scale necessary. This of course does not exclude the possibility that there is a cortical feedback mechanism involving the indirect corticoreticular thalamic route to make use of long inhibitory synaptic time-scales to reinitiate burst generation.

Intrinsic mechanisms based on a pace-making cation current that repolarizes the thalamic neurons is a feasible mechanism for the rhythmic nature of LTS bursts in TCD. However, this mechanism is highly sensitive to noise, since the current generated by these ion-channels is rather weak.

The most robust mechanism seems to be the short feedback loop via the reticular thalamic nucleus. This circuit has been investigated extensively in the context of sleep rhythms and has been shown to be physiological and robust at the same time. It has also been shown experimentally that such a circuit can engage in the generation of slow sleep oscillations that are similar in frequency to the oscillations observed in TCD.

It is likely that in the biological thalamus different mechanisms interact. Specifically, the intrinsic bursting mechanism could trigger TCD rhythms in the case of thalamic hyperpolarization that then subsequently gets augmented with the more stable inhibitory reticular feedback mechanism. With a combination of two mechanisms one could combine the simplicity of intrinsic bursting with the robustness of neuronal feedback circuits.

Thalamic networks and the effect of functional neurosurgery

In Chapter 4 the behavior of thalamic cell ensembles has been investigated under TCD conditions. Network models are generally harder to setup and control than the single circuit model presented in Chapter 3. In spite of that, our model shows remarkable stability. As predicted by TCD theory a simple deafferentation of a portion of thalamic afferent fibers can lead to the generation of calcium bursts. This is mediated by the relation of thresholds in thalamic reticular neurons. Our model predicts that a decrease in excitatory input can effectively hyperpolarize these neurons and lead to the generation of calcium bursts if the RTN neurons get depolarized by sporadic cortical or thalamic excitation. The increase in burst

incidence in RTN can then recruit rebound bursts especially in the non-specific nuclei of the thalamus of which the central lateral nucleus is a prime example. This is caused by the particularly dense innervation from RTN to NSP, leading to the generation of limit-cycle behavior between those nuclei in the way described in Chapter 3. The specific parts of the thalamus play only a small role in the generation of pathological rhythmicity and stay largely unaffected by the change in NSP/RTN behavior - apart from the directly deafferented areas.

Our model is then able to explain the effect that stereotactic neurosurgery has on the TCD patient. Our model predicts that the pacemaking mechanism is seated in the NSP-RTN circuitry and that a lesion will be effective if most of the deafferented neurons get coagulated. This is in accordance with the finding that the posterior part of CL not only has the highest burst-incidence in TCD patients but is also the most effective surgical target.

Cortical feedback is neglected in our model for reasons of simplicity. However, our bursting mechanism is completely compatible with the introduction of cortical feedback loops whose activity is influenced in part by the afferent input from the thalamus. The entrainment of cortical areas will further decrease afferent thalamic excitation making hyperpolarization triggered bursting all the more likely.

Our model also has some interesting implications with regards to the unification of psychological and physiological brain disorders. The CL and similar thalamic nuclei are highly non-specific in their innervation as they receive input from a wide variety of cortical areas, from specific primary sensory areas to paralimbic areas associated with emotional control. It is this interface in which the interaction between neurological disorders and the emotional state of the patient can take place. Lack of excitation in the related RTN areas can be mediated by both peripheral deafferentation but also changes to paralimbic activity. In this scheme the affective and biophysical dimensions of neurological disorders exist along the same spectrum.

Along the same lines, I was able to extrapolate to other treatments of dynamical brain disorders such as Ramachandran's mirror box in which excitation of deafferented areas by means of multimodal stimulation is an effective treatment for neurogenic pain in the TCD context.

TCD-caused cortical deinhibition

Lastly, in Chapter 5 I have looked at the mechanisms leading to the production of positive symptoms in patients suffering from TCD. It has long been recognized that thalamic low-frequency reduction can not in itself be responsible for

the manifestations of positive symptoms associated with TCD. Llinas et al. have postulated an edge effect [77, 78] in which local low-frequency stimulation of cortex disbalances the inherent excitatory-inhibitory equilibrium leading to lateral disinhibition and hence a halo of overactivation around the region affected by the TCD. This overactivation can then cause symptoms like tremor, pain and tinnitus that by their very nature require an excess of activity to occur. Evidence for this effect in vivo or in vitro has been sparse [78], since there are at present no good animal models of TCD. I built two models in order to investigate what parameters would make such a mechanism feasible:

I firstly modeled cortex as a continuum of homogeneous units - comparable to cortical microcolumns - that were laterally connected in a realistic excitatory-inhibitory profile. The edge effect was clearly visible from the start as long as cortical excitation exceeded cortical inhibition in range.

I sought to extend these results with a more biologically plausible spiking neuron model. Again, I was able to produce significant edge effects in TCD conditions. This relied again on the exact profile of excitation and inhibition and in addition on the cell dynamics implemented in the model. We found that fast-spiking inhibitory neurons are more potent in producing edges than the more generic regular-spiking cell type featuring adaptation.

These results predict that the edge effect relies exclusively in an initial imbalance of excitation and inhibition that is then exacerbated by the TCD. If all parameters are equal a dysrhythmia will cause lateral deinhibition as well as lateral deexcitation. In my models, I made use of the particular differences found in the cortical connectivity architectures. Furthermore, a difference in single neuron dynamics can also be the cause of such an imbalance. Under the normal high frequency stimulation regime fast-spiking inhibitory interneurons are more effective relative to regular-spiking excitatory neurons than under low-frequency (TCD) stimulation. Hence the inhibitory neurons are more affected creating the deinhibition necessary for an edge effect.

In fact, if excitatory neurons were modeled as regular-spiking and inhibitory neurons were modeled as fast-spiking an edge effect was measurable under all connectivity profiles.

Plasticity

A question we were as yet unable to address is concerned with the involvement of plastic changes in cortical connectivity in response to prolonged thalamocortical dysrhythmia. Surgical relief of symptoms in TCD tends to occur over a relatively long time-scale, from days to weeks, and large-scale physiological

measures like EEG/MEG take up to 12 months to recover from the pathological state [129]. This indicates that a significant amount of plastic changes have to take place from the onset of the disease to surgical lesion of the central lateral nucleus or the pallidothalamic tract.

One feasible mechanism that would allow for such a slow recovery from the pathological state involves Hebbian learning in and around the TCD-affected cortical area. Overactive regions are likely to increase synaptic weights between each other, because of an increased probability of concurrent activity, strengthening the edge. Over a prolonged period of time this can then lead from short-term synaptic changes to changes in the morphology leading to long recovery times relating to the individual plasticity of the patient's brain.

6.2 Conclusions

In conclusion, in this work we have provided theoretical evidence corroborating the notion that dysrhythmic brain states can serve as a general description of functional neurological disease. This allows us to propose a unified approach to brain disorders targeting the dysrhythmic pacemakers. The understanding of such a system will become increasingly valuable in the coming years with the arrival of focussed ultrasound minimally invasive techniques that allow a further reduction of intra-operative risk by means of increasing precision and decreasing invasiveness.

In building a numerical model of TCD we have been able to elucidate some of the mechanisms previously predicted by abstract theoretical modeling of the disease and were able to generate testable predictions.

The thalamus is above all a neuronal rhythm machine that is inherently sensitive to changes in afferent input statistics. At the same time the thalamus provides an interface of all areas of the brain in a small nucleus allowing for multimodal interactions of different brain systems. Our model shows the potential effects that both conventional pharmaceutical and surgical therapy as well as psychological therapeutical techniques can have on the thalamus, in particular the medial thalamic nuclei.

Appendix A

Model Parameters

The following tables show the parameters used in the thalamic models of Chapters 3 and 4:

	RTN	SP	NSP
Spiking Threshold (mV)	-35	-35	-35
Vm Reset (mV)	-50	-50	-50
Leak Conductance (mS)	0.035	0.035	0.035
Leak Reversal (mV)	-65	-65	-65
T Conductance (mS)	0.07	0.07	0.07
T Threshold (mV)	-64	-66	-66
τ_h depolarized (ms)	40	20	20
τ_h hyperpolarized (ms)	100	100	100

Table A.1: Neuron model parameters.

	type	τ	weight	arborization	probability
SP input → SP	excitatory	10	0.005	1-to-1	1
NSP input → NSP	excitatory	10	0.005	1-to-1	1
CRX input → CRX	excitatory	7	0.01	1-to-1	1
SP → RTN	excitatory	20	0.02	1-to-1	1
NSP → RTN	excitatory	20	0.01	seed1	0.15
RTN → SP	inhibitory	30	0.03	1-to-1	1
RTN → NSP	inhibitory	30	0.02	seed1	0.15

Table A.2: Connectivity parameters.

	awake	sleep	TCD
SP input (ms^{-1})	0.5	0.3	0.5
NSP input (ms^{-1})	0.5	0.4	0.5
CRX input (ms^{-1})	0.15	0.01	0.15

Table A.3: Input parameters.

Bibliography

[1] E. D. Adrian. Afferent discharges to the cerebral cortex from peripheral sense organs. *J Physiol*, 100(2):159–191, Sep 1941.

[2] Jose-Manuel Alonso and Harvey A Swadlow. Thalamocortical specificity and the synthesis of sensory cortical receptive fields. *J Neurophysiol*, 94(1):26–32, Jul 2005.

[3] P. Andersen and J. Eccles. Inhibitory phasing of neuronal discharge. *Nature*, 196:645–647, Nov 1962.

[4] J. D. Angstadt and R. L. Calabrese. A hyperpolarization-activated inward current in heart interneurons of the medicinal leech. *J Neurosci*, 9(8):2846–2857, Aug 1989.

[5] C. Aufenberg, J. Sarnthein, A. Morel, V. Rousson, M. Gallay, and D. Jeanmonod. A revival of spiegel's campotomy: long term results of the stereotactic pallidothalamic tractotomy against the parkinsonian thalamocortical dysrhythmia. *Thalamus & Related Systems*, 3:121–132, 2005.

[6] E. Basar. *Dynamics of Sensory and Cognitive Processing by the Brain*, volume 1 of *Springer Series in Brain Dynamics*, chapter EEG-brain dynamics. Relation between EEG and Brain Evoked Potentials, pages 30–55. Elsevier: Amsterdam, NL, 1988.

[7] M. Bazhenov, I. Timofeev, M. Steriade, and T. J. Sejnowski. Self-sustained rhythmic activity in the thalamic reticular nucleus mediated by depolarizing GABAA receptor potentials. *Nat Neurosci*, 2(2):168–174, Feb 1999.

[8] Maxim Bazhenov, Igor Timofeev, Mircea Steriade, and Terrence J Sejnowski. Model of thalamocortical slow-wave sleep oscillations and transitions to activated states. *J Neurosci*, 22(19):8691–8704, Oct 2002.

[9] Hans Berger. Über das elektrenkephalogramm des menschen. *Arch Psychiatr Nervenkr*, 87:527–570, 1929.

[10] G. E. Berrios. Positive and negative symptoms and jackson. a conceptual history. *Arch Gen Psychiatry*, 42(1):95–97, Jan 1985.

[11] G. H. Bishop. The interpretation of cortical potentials. *Cold Spring Harbor Symp Quant Biol*, 4:305–319, 1936.

[12] H. Blumenfeld and D. A. McCormick. Corticothalamic inputs control the pattern of activity generated in thalamocortical networks. *J Neurosci*, 20(13):5153–5162, Jul 2000.

[13] J. Boivie. The termination of the spinothalamic tract in the cat. an experimental study with silver impregnation methods. *Exp Brain Res*, 112(4):331–353, May 1971.

[14] F. Bremer. Effets de la déafférentation complète d'une région de lécorce cérébrale sur son activité électrique spontanée. *C. R. Soc. Biol. (Paris)*, 127:355–359, 1938.

[15] Randy M Bruno and Bert Sakmann. Cortex is driven by weak but synchronously active thalamocortical synapses. *Science*, 312(5780):1622–1627, Jun 2006.

[16] G. Buzsaki, R. G. Bickford, G. Ponomareff, L. J. Thal, R. Mandel, and F. H. Gage. Nucleus basalis and thalamic control of neocortical activity in the freely moving rat. *J Neurosci*, 8(11):4007–4026, Nov 1988.

[17] G. Buzsaki and A. Draguhn. Neuronal oscillations in cortical networks. *Science*, 304(5679):1926–9, 2004.

[18] G. Buzsáki. The thalamic clock: emergent network properties. *Neuroscience*, 41(2-3):351–364, 1991.

[19] G. Buzsáki, A. Smith, S. Berger, L. J. Fisher, and F. H. Gage. Petit mal epilepsy and parkinsonian tremor: hypothesis of a common pacemaker. *Neuroscience*, 36(1):1–14, 1990.

[20] Rudy Capildeo. *Movement Disorders: Tremor*, chapter Rebound excitation as the physiological basis for tremor: a biophysical study of the oscillatory properties of mammlian central neurones in vitro, pages 165–183. The Macmillan Press Ltd.: London, 1984.

[21] E. Carbone and H. D. Lux. A low voltage-activated calcium conductance in embryonic chick sensory neurons. *Biophys J*, 46(3):413–418, Sep 1984.

[22] E. Carbone and H. D. Lux. A low voltage-activated, fully inactivating ca channel in vertebrate sensory neurones. *Nature*, 310(5977):501–502, 1984.

[23] P. Cesaro, M. W. Mann, J. L. Moretti, G. Defer, B. Roualdés, J. P. Nguyen, and J. D. Degos. Central pain and thalamic hyperactivity: a single photon emission computerized tomographic study. *Pain*, 47(3):329–336, Dec 1991.

[24] Albert Compte, Maria V Sanchez-Vives, David A McCormick, and Xiao-Jing Wang. Cellular and network mechanisms of slow oscillatory activity (¡1 Hz) and wave propagations in a cortical network model. *J Neurophysiol*, 89(5):2707–2725, May 2003.

[25] D. Contreras, A. Destexhe, T. J. Sejnowski, and M. Steriade. Control of spatiotemporal coherence of a thalamic oscillation by corticothalamic feedback. *Science*, 274(5288):771–774, Nov 1996.

[26] Diego Contreras. The role of t-channels in the generation of thalamocortical rhythms. *CNS Neurol Disord Drug Targets*, 5(6):571–585, Dec 2006.

[27] R. Curo-Dossi, A. Nuñez, and M. Steriade. Electrophysiology of a slow (0.5-4 hz) intrinsic oscillation of cat thalamocortical neurones in vivo. *J Physiol*, 447:215–234, Feb 1992.

[28] M. S. Dekin. Inward rectification and its effects on the repetitive firing properties of bulbospinal neurons located in the ventral part of the nucleus tractus solitarius. *J Neurophysiol*, 70(2):590–601, Aug 1993.

[29] Ysbrand D Van der Werf, Menno P Witter, and Henk J Groenewegen. The intralaminar and midline nuclei of the thalamus. Anatomical and functional evidence for participation in processes of arousal and awareness. *Brain Res Brain Res Rev*, 39(2-3):107–140, Sep 2002.

[30] M. Deschênes, A. Madariaga-Domich, and M. Steriade. Dendrodendritic synapses in the cat reticularis thalami nucleus: a structural basis for thalamic spindle synchronization. *Brain Res*, 334(1):165–168, May 1985.

[31] M. Deschênes, M. Paradis, J. P. Roy, and M. Steriade. Electrophysiology of neurons of lateral thalamic nuclei in cat: resting properties and burst discharges. *J Neurophysiol*, 51(6):1196–1219, Jun 1984.

[32] A. Destexhe and A. Babloyantz. A model of the inward current Ih and its possible role in thalamocortical oscillations. *Neuroreport*, 4(2):223–226, Feb 1993.

[33] A. Destexhe, A. Babloyantz, and T. J. Sejnowski. Ionic mechanisms for intrinsic slow oscillations in thalamic relay neurons. *Biophys J*, 65(4):1538–52, 1993.

[34] A. Destexhe, T. Bal, D. A. McCormick, and T. J. Sejnowski. Ionic mechanisms underlying synchronized oscillations and propagating waves in a model of ferret thalamic slices. *J Neurophysiol*, 76(3):2049–2070, Sep 1996.

[35] A. Destexhe, D. Contreras, T. J. Sejnowski, and M. Steriade. A model of spindle rhythmicity in the isolated thalamic reticular nucleus. *J Neurophysiol*, 72(2):803–818, Aug 1994.

[36] A. Destexhe, D. Contreras, T. J. Sejnowski, and M. Steriade. Modeling the control of reticular thalamic oscillations by neuromodulators. *Neuroreport*, 5(17):2217–2220, Nov 1994.

[37] A. Destexhe, D. A. McCormick, and T. J. Sejnowski. A model for 8-10 hz spindling in interconnected thalamic relay and reticularis neurons. *Biophys J*, 65(6):2473–7, 1993.

[38] A. Destexhe and T. J. Sejnowski. The initiation of bursts in thalamic neurons and the cortical control of thalamic sensitivity. *Philos Trans R Soc Lond B Biol Sci*, 357(1428):1649–57, 2002.

[39] A. Destexhe and T. J. Sejnowski. Interactions between membrane conductances underlying thalamocortical slow-wave oscillations. *Physiol Rev*, 83(4):1401–53, 2003.

[40] R. J. Douglas and K. A. Martin. Neuronal circuits of the neocortex. *Annu Rev Neurosci*, 27:419–51, 2004.

[41] Pascal Fries. A mechanism for cognitive dynamics: neuronal communication through neuronal coherence. *Trends Cogn Sci*, 9(10):474–480, Oct 2005.

[42] T. L. Frigyesi. Intracellular recordings from neurons in dorsolateral thalamic reticular nucleus druring capsular, basal ganglia and midline thalamic stimulation. *Brain Research*, pages 157–172, 1972.

[43] Leon Glass. Synchronization and rhythmic processes in physiology. *Nature*, 410:277–284, 2001.

[44] D. Golomb, X. J. Wang, and J. Rinzel. Synchronization properties of spindle oscillations in a thalamic reticular nucleus model. *J Neurophysiol*, 72(3):1109–1126, Sep 1994.

[45] C. M. Gray. Synchronous oscillations in neuronal systems: mechanisms and functions. *J Comput Neurosci*, 1(1-2):11–38, Jun 1994.

[46] H. J. Groenewegen and H. W. Berendse. The specificity of the 'non-specific' midline and intralaminar thalamic nuclei. *Trends Neurosci*, 17(2):52–57, Feb 1994.

[47] R. W. Guillery and J. K. Harting. Structure and connections of the thalamic reticular nucleus: Advancing views over half a century. *J Comp Neurol*, 463(4):360–71, 2003.

[48] R. M. Harris. Axon collaterals in the thalamic reticular nucleus from thalamocortical neurons of the rat ventrobasal thalamus. *J Comp Neurol*, 258(3):397–406, Apr 1987.

[49] H. K. Hartline, H. G. Wagner, and F. Ratliff. Inhibition in the eye of Limulus. *J Gen Physiol*, 39(5):651–673, May 1956.

[50] H. Head and G. Holmes. Sensory disturbances from cerebral lesions. *Brain*, 34:102–254, 1911.

[51] S. M. Hersch and E. L. White. Thalamocortical synapses with corticothalamic projection neurons in mouse smi cortex: electron microscopic demonstration of a monosynaptic feedback loop. *Neurosci Lett*, 24(3):207–210, Jul 1981.

[52] H. Hinrichs and W. Machleidt. Basic emotions reflected in EEG-coherences. *Int J Psychophysiol*, 13(3):225–232, Dec 1992.

[53] A. L. Hodgkin and A. F. Huxley. A quantitative description of membrane current and its application to conduction and excitation in nerve. *J Physiol*, 117(4):500–544, Aug 1952.

[54] C. R. Houser, J. E. Vaughn, R. P. Barber, and E. Roberts. GABA neurons are the major cell type of the nucleus reticularis thalami. *Brain Res*, 200(2):341–354, Nov 1980.

[55] Stuart W Hughes and Vincenzo Crunelli. Thalamic mechanisms of eeg alpha rhythms and their pathological implications. *Neuroscientist*, 11(4):357–372, Aug 2005.

[56] J. R. Huguenard and D. A. McCormick. Simulation of the currents involved in rhythmic oscillations in thalamic relay neurons. *J Neurophysiol*, 68(4):1373–1383, Oct 1992.

[57] J. R. Huguenard and D. A. Prince. A novel t-type current underlies prolonged ca(2+)-dependent burst firing in gabaergic neurons of rat thalamic reticular nucleus. *J Neurosci*, 12(10):3804–17, 1992.

[58] Eugene M. Izhikevich. Simple model of spiking neurons. *IEEE Trans Neural Netw*, 14:1569–1572, 2003.

[59] Eugene M Izhikevich. Polychronization: computation with spikes. *Neural Comput*, 18(2):245–282, Feb 2006.

[60] Eugene M Izhikevich, Joseph A Gally, and Gerald M Edelman. Spike-timing dynamics of neuronal groups. *Cereb Cortex*, 14(8):933–944, Aug 2004.

[61] H. Jahnsen and R. Llinás. Ionic basis for the electro-responsiveness and oscillatory properties of guinea-pig thalamic neurones in vitro. *J Physiol*, 349:227–247, Apr 1984.

[62] D. Jeanmonod, M. Magnin, and A. Morel. Thalamus and neurogenic pain: physiological, anatomical and clinical data. *Neuroreport*, 4(5):475–8, 1993.

[63] D. Jeanmonod, M. Magnin, and A. Morel. Low-threshold calcium spike bursts in the human thalamus. common physiopathology for sensory, motor and limbic positive symptoms. *Brain*, 119(2):363–75, 1996.

[64] D. Jeanmonod, M. Magnin, A. Morel, and M. Siegemund. Surgical control of the human thalamocortical dysrhythmia. part i. central lateral thalamotomy in neurogenic pain. *Thalamus & Related Systems*, 1:71–79, 2001.

[65] D. Jeanmonod, M. Magnin, A. Morel, M. Siegemund, R. Cancro, M. Lanz, R. Llinas, U. Ribary, E. Kronberg, J. Schulman, and M. Zonenshayn. Thalamocortical dysrhythmia ii. clinical and surgical aspects. *Thalamus and Related Systems*, 1:245–254, 2001.

[66] D. Jeanmonod, J. Schulman, R. Ramirez, R. Cancro, M. Lanz, A. Morel, M. Magnin, M. Siegemund, E. Kronberg, U. Ribary, and R. Llinas. Neuropsychiatric thalamocortical dysrhythmia: surgical implications. *Neurosurg Clin N Am*, 14(2):251–65, 2003.

[67] E. G. Jones. Some aspects of the organization of the thalamic reticular complex. *J Comp Neurol*, 162(3):285–308, Aug 1975.

[68] E. G. Jones. Thalamic circuitry and thalamocortical synchrony. *Philos Trans R Soc Lond B Biol Sci*, 357(1428):1659–73, 2002.

[69] Edward G. Jones. *The Thalamus Revisited*. Cambridge, UK. Cambridge University Press, 2006.

[70] U. Kim, M. V. Sanchez-Vives, and D. A. McCormick. Functional dynamics of gabaergic inhibition in the thalamus. *Science*, 278(5335):130–134, Oct 1997.

[71] F. A. Lenz, H. C. Kwan, J. O. Dostrovsky, and R. R. Tasker. Characteristics of the bursting pattern of action potentials that occurs in the thalamus of patients with central pain. *Brain Res*, 496(1-2):357–60, 1989.

[72] X. B. Liu, C. N. Honda, and E. G. Jones. Distribution of four types of synapse on physiologically identified relay neurons in the ventral posterior thalamic nucleus of the cat. *J Comp Neurol*, 352(1):69–91, 1995.

[73] Xiao-Bo Liu and Edward G Jones. Fine structural localization of connexin-36 immunoreactivity in mouse cerebral cortex and thalamus. *J Comp Neurol*, 466(4):457–467, Nov 2003.

[74] M. S. Livingstone and D. H. Hubel. Effects of sleep and arousal on the processing of visual information in the cat. *Nature*, 291(5816):554–561, Jun 1981.

[75] R. Llinas and H. Jahnsen. Electrophysiology of mammalian thalamic neurones in vitro. *Nature*, 297(5865):406–8, 1982.

[76] R. Llinas, U. Ribary, D. Jeanmonod, R. Cancro, E. Kronberg, J. Schulman, M. Zonenshayn, M. Magnin, A. Morel, and M. Siegemund. Thalamocortical dysrhythmia i. functional and imaging aspects. *Thalamus and Related Systems*, 1:237–244, 2001.

[77] R. R. Llinas, U. Ribary, D. Jeanmonod, E. Kronberg, and P. P. Mitra. Thalamocortical dysrhythmia: A neurological and neuropsychiatric syndrome characterized by magnetoencephalography. *Proc Natl Acad Sci U S A*, 96(26):15222–7, 1999.

[78] Rodolfo Llinás, Francisco J Urbano, Elena Leznik, Rey R Ramírez, and Hein J F van Marle. Rhythmic and dysrhythmic thalamocortical dynamics: GABA systems and the edge effect. *Trends Neurosci*, 28(6):325–333, Jun 2005.

[79] I. P. Lukashevich and O. B. Sazonova. [the effect of lesions of different parts of the optic thalamus on the nature of the bioelectrical activity of the human brain]. *Zh Vyssh Nerv Deiat Im I P Pavlova*, 46(5):866–874, 1996.

[80] W. W. Lytton, A. Destexhe, and T. J. Sejnowski. Control of slow oscillations in the thalamocortical neuron: a computer model. *Neuroscience*, 70(3):673–684, Feb 1996.

[81] W. Machleidt, L. Gutjahr, and A. Mügge. [basic emotions. phenomenology, psychodynamics, eeg spectral analysis]. *Monogr Gesamtgeb Psychiatr Psychiatry Ser*, 57:1–251, 1989.

[82] M. Magnin, D. Jeanmonod, A. Morel, and M. Siegemund. Surgical control of the human thalamocortical dysrhythmia. part ii. pallidothalamic tractotomy in parkinson's disease. *Thalamus & Related Systems*, 1:81–89, 2001.

[83] M. Magnin, A. Morel, and D. Jeanmonod. Single-unit analysis of the pallidum, thalamus and subthalamic nucleus in parkinsonian patients. *Neuroscience*, 96(3):549–564, 2000.

[84] Kerry McAlonan, James Cavanaugh, and Robert H Wurtz. Attentional modulation of thalamic reticular neurons. *J Neurosci*, 26(16):4444–4450, Apr 2006.

[85] Kerry McAlonan, James Cavanaugh, and Robert H Wurtz. Guarding the gateway to cortex with attention in visual thalamus. *Nature*, 456(7220):391–394, Nov 2008.

[86] D. A. McCormick and J. R. Huguenard. A model of the electrophysiological properties of thalamocortical relay neurons. *J Neurophysiol*, 68(4):1384–1400, Oct 1992.

[87] D. A. McCormick and H. C. Pape. Properties of a hyperpolarization-activated cation current and its role in rhythmic oscillation in thalamic relay neurones. *J Physiol*, 431:291–318, Dec 1990.

[88] G. W. Milton. Self-willed death or the bone-pointing syndrome. *Lancet*, 1(7817):1435–1436, Jun 1973.

[89] Morteza Moazami-Goudarzi, Johannes Sarnthein, Lars Michels, Renata Moukhtieva, and Daniel Jeanmonod. Enhanced frontal low and high frequency power and synchronization in the resting eeg of parkinsonian patients. *Neuroimage*, 41(3):985–997, Jul 2008.

[90] L. M. Modesti and M. Waszak. Firing pattern of cells in human thalamus during dorsal column stimulation. *Appl Neurophysiol*, 38(4):251–258, 1975.

[91] C. Mulle, A. Madariaga, and M. Deschênes. Morphology and electrophysiological properties of reticularis thalami neurons in cat: in vivo study of a thalamic pacemaker. *J Neurosci*, 6(8):2134–2145, Aug 1986.

[92] V. N. Murthy and E. E. Fetz. Oscillatory activity in sensorimotor cortex of awake monkeys: synchronization of local field potentials and relation to behavior. *J Neurophysiol*, 76(6):3949–3967, Dec 1996.

[93] A. Nuñez, R. Curró Dossi, D. Contreras, and M. Steriade. Intracellular evidence for incompatibility between spindle and delta oscillations in thalamocortical neurons of cat. *Neuroscience*, 48(1):75–85, 1992.

[94] P. T. Ohara and A. R. Lieberman. Thalamic reticular nucleus: anatomical evidence that cortico-reticular axons establish monosynaptic contact with reticulo-geniculate projection cells. *Brain Res*, 207(1):153–156, Feb 1981.

[95] P. T. Ohara and A. R. Lieberman. The thalamic reticular nucleus of the adult rat: experimental anatomical studies. *J Neurocytol*, 14(3):365–411, Jun 1985.

[96] T. Ohmoto, Y. Mimura, Y. Baba, T. Miyamoto, Y. Matsumoto, A. Nishimoto, and K. Matsumoto. Thalamic control of spontaneous alpha-rhythm and evoked responses. *Appl Neurophysiol*, 41(1-4):188–192, 1978.

[97] World Health Organization. *Neurological Disorders: Public Health Challenges*. WHO Press: Geneva, CH, 2006.

[98] H. C. Pape. Queer current and pacemaker: the hyperpolarization-activated cation current in neurons. *Annu Rev Physiol*, 58:299–327, 1996.

[99] Alejandro Pascual, Julien Modolo, and Anne Beuter. Is a computational model useful to understand the effect of deep brain stimulation in parkinson's disease? *J Integr Neurosci*, 5(4):541–559, Dec 2006.

[100] S. N. Raeva, N. Ia Vasin, V. A. Shabalov, M. R. Medzhidov, and V. V. Shashkov. [identification of nuclei of the pretectal area during stereotaxic surgery for spastic torticollis]. *Zh Vopr Neirokhir Im N N Burdenko*, (5):39–43, 1986.

[101] V. S. Ramachandran and D. Rogers-Ramachandran. Synaesthesia in phantom limbs induced with mirrors. *Proc Biol Sci*, 263(1369):377–386, Apr 1996.

[102] E. J. Ramcharan, J. W. Gnadt, and S. M. Sherman. Higher-order thalamic relays burst more than first-order relays. *Proc Natl Acad Sci U S A*, 102(34):12236–41, 2005.

[103] P. Reinagel and R. C. Reid. Temporal coding of visual information in the thalamus. *J Neurosci*, 20(14):5392–5400, Jul 2000.

[104] U. Ribary, A. A. Ioannides, K. D. Singh, R. Hasson, J. P. Bolton, F. Lado, A. Mogilner, and R. Llinas. Magnetic field tomography of coherent thalamocortical 40-hz oscillations in humans. *Proc Natl Acad Sci U S A*, 88(24):11037–11041, Dec 1991.

[105] P. C. Rinaldi, R. F. Young, D. Albe-Fessard, and J. Chodakiewitz. Spontaneous neuronal hyperactivity in the medial and intralaminar thalamic nuclei of patients with deafferentation pain. *J Neurosurg*, 74(3):415–421, Mar 1991.

[106] C. Roth, D. Jeanmonod, M. Magnin, A. Morel, and P. Achermann. Effects of medial thalamotomy and pallido-thalamic tractotomy on sleep and waking eeg in pain and parkinsonian patients. *Clin Neurophysiol*, 111(7):1266–75, 2000.

[107] Jonathan E Rubin and David Terman. High frequency stimulation of the subthalamic nucleus eliminates pathological thalamic rhythmicity in a computational model. *J Comput Neurosci*, 16(3):211–235, 2004.

[108] K. Sano. Intralaminar thalamotomy (thalamolaminotomy) and posteromedial hypothalamotomy in the treatment of intractable pain. *Progress in Neurological Surgery*, 8:50–103, 1977.

[109] J. Sarnthein, A. Morel, A. von Stein, and D. Jeanmonod. Thalamic theta field potentials and eeg: high thalamocortical coherence in patients with neurogenic pain, epilepsy and movement disorders. *Thalamus & Related Systems*, 2:231–238, 2003.

[110] J. Sarnthein, A. Morel, A. von Stein, and D. Jeanmonod. Thalamocortical theta coherence in neurological patients at rest and during a working memory task. *Int J Psychophysiol*, 57(2):87–96, 2005.

[111] J. Sarnthein, J. Stern, C. Aufenberg, V. Rousson, and D. Jeanmonod. Increased eeg power and slowed dominant frequency in patients with neurogenic pain. *Brain*, 129(Pt 1):55–64, 2006.

[112] Johannes Sarnthein and Daniel Jeanmonod. High thalamocortical theta coherence in patients with parkinson's disease. *J Neurosci*, 27(1):124–131, Jan 2007.

[113] S. M. Sherman. A wake-up call from the thalamus. *Nat Neurosci*, 4(4):344–6, 2001.

[114] S. Murray Sherman. The thalamus is more than just a relay. *Curr Opin Neurobiol*, Aug 2007.

[115] A. Shosaku, Y. Kayama, I. Sumitomo, M. Sugitani, and K. Iwama. Analysis of recurrent inhibitory circuit in rat thalamus: neurophysiology of the thalamic reticular nucleus. *Prog Neurobiol*, 32(2):77–102, 1989.

[116] W. Singer. Synchronization of cortical activity and its putative role in information processing and learning. *Annu Rev Physiol*, 55:349–374, 1993.

[117] G. D. Smith, C. L. Cox, S. M. Sherman, and J. Rinzel. Fourier analysis of sinusoidally driven thalamocortical relay neurons and a minimal integrate-and-fire-or-burst model. *J Neurophysiol*, 83(1):588–610, 2000.

[118] Vikaas S Sohal, Susanne Pangratz-Fuehrer, Uwe Rudolph, and John R Huguenard. Intrinsic and synaptic dynamics interact to generate emergent patterns of rhythmic bursting in thalamocortical neurons. *J Neurosci*, 26(16):4247–4255, Apr 2006.

[119] M. Steriade. Synchronized activities of coupled oscillators in the cerebral cortex and thalamus at different levels of vigilance. *Cereb Cortex*, 7(6):583–604, Sep 1997.

[120] M. Steriade. To burst, or rather, not to burst. *Nat Neurosci*, 4(7):671, Jul 2001.

[121] M. Steriade. Grouping of brain rhythms in corticothalamic systems. *Neuroscience*, 137(4):1087–1106, 2006.

[122] M. Steriade and M. Deschenes. The thalamus as a neuronal oscillator. *Brain Res*, 320(1):1–63, 1984.

[123] M. Steriade, M. Deschenes, L. Domich, and C. Mulle. Abolition of spindle oscillations in thalamic neurons disconnected from nucleus reticularis thalami. *J Neurophysiol*, 54(6):1473–97, 1985.

[124] M. Steriade, L. Domich, and G. Oakson. Reticularis thalami neurons revisited: activity changes during shifts in states of vigilance. *J Neurosci*, 6(1):68–81, Jan 1986.

[125] M. Steriade, E. G. Jones, and R. Llinas. *Thalamic Oscillations and Signaling*. Wiley-Liss, New York, 1990.

[126] M. Steriade, D. A. McCormick, and T. J. Sejnowski. Thalamocortical oscillations in the sleeping and aroused brain. *Science*, 262(5134):679–685, Oct 1993.

[127] M. Steriade, A. Parent, and J. Hada. Thalamic projections of nucleus reticularis thalami of cat: a study using retrograde transport of horseradish peroxidase and fluorescent tracers. *J Comp Neurol*, 229(4):531–547, Nov 1984.

[128] Mircea Steriade. Sleep, epilepsy and thalamic reticular inhibitory neurons. *Trends Neurosci*, 28(6):317–324, Jun 2005.

[129] Jair Stern, Daniel Jeanmonod, and Johannes Sarnthein. Persistent EEG overactivation in the cortical pain matrix of neurogenic pain patients. *Neuroimage*, 31(2):721–731, Jun 2006.

[130] M. Stopfer, S. Bhagavan, B. H. Smith, and G. Laurent. Impaired odour discrimination on desynchronization of odour-encoding neural assemblies. *Nature*, 390(6655):70–74, Nov 1997.

[131] Y. Terao, Y. Sakurai, M. Sakuta, K. Ishii, and M. Sugishita. [fdg-pet in an amnestic and hypersomnic patient with bilateral paramedian thalamic infarction]. *Rinsho Shinkeigaku*, 33(9):951–956, Sep 1993.

[132] Roger D Traub, Diego Contreras, Mark O Cunningham, Hilary Murray, Fiona E N LeBeau, Anita Roopun, Andrea Bibbig, W. Bryan Wilent, Michael J Higley, and Miles A Whittington. Single-column thalamocortical network model exhibiting gamma oscillations, sleep spindles, and epileptogenic bursts. *J Neurophysiol*, 93(4):2194–2232, Apr 2005.

[133] M. von Krosigk, T. Bal, and D. A. McCormick. Cellular mechanisms of a synchronized oscillation in the thalamus. *Science*, 261(5119):361–364, Jul 1993.

[134] G. V. Wallenstein. A model of the electrophysiological properties of nucleus reticularis thalami neurons. *Biophys J*, 66(4):978–988, Apr 1994.

[135] Ralf Weigel and Joachim K Krauss. Center median-parafascicular complex and pain control. review from a neurosurgical perspective. *Stereotact Funct Neurosurg*, 82(2-3):115–126, 2004.

[136] T. G. Weyand, M. Boudreaux, and W. Guido. Burst and tonic response modes in thalamic neurons during sleep and wakefulness. *J Neurophysiol*, 85(3):1107–1118, Mar 2001.

[137] E. L. White and S. M. Hersch. A quantitative study of thalamocortical and other synapses involving the apical dendrites of corticothalamic projection cells in mouse smi cortex. *J Neurocytol*, 11(1):137–157, Feb 1982.

[138] Reto Wyss, Peter König, and Paul F M J Verschure. Invariant representations of visual patterns in a temporal population code. *Proc Natl Acad Sci U S A*, 100(1):324–329, Jan 2003.

[139] Reto Wyss, Peter König, and Paul F M J Verschure. A model of the ventral visual system based on temporal stability and local memory. *PLoS Biol*, 4(5):e120, May 2006.

[140] J. Xing and G. L. Gerstein. Networks with lateral connectivity. I. dynamic properties mediated by the balance of intrinsic excitation and inhibition. *J Neurophysiol*, 75(1):184–199, Jan 1996.

[141] C. T. Yen, M. Conley, S. H. Hendry, and E. G. Jones. The morphology of physiologically identified gabaergic neurons in the somatic sensory part of the thalamic reticular nucleus in the cat. *J Neurosci*, 5(8):2254–2268, Aug 1985.